List of Figures

List of Figures

List of Tables

1. INTRODUCTION

NASA and RSC-E are involved in a cooperative venture in which the Shuttle will rendezvous with the Mir Space Station during several missions over the next three years. This sequence of at least six missions will serve as a precursor to the two nations' involvement in the International Space Station. The rendezvous missions provide NASA and RSC-E scientists and engineers an excellent opportunity to study the orbital, dynamic, and environmental conditions of long duration spacecraft, as well as the opportunity to develop evaluation and risk mitigation techniques which have direct application to the International Space Station.

STS-71 was the Shuttle's first docking mission with the Mir station. Approximately 670 photographs and 24 hours of video of the Mir station were acquired during the rendezvous. This report documents results from several survey-related analysis tasks.

Results of the DTO-1118 analysis from STS-63 were documented in an earlier report. The STS-63 JSC/RSC-E Mir Survey Joint Report is currently in distribution.

1.1 Overview of Mir Photo/TV Survey

Detailed Test Objective (DTO-1118) integrates the requirements for photographic and video imagery of the Mir Space Station generated by the engineering and science communities in NASA.

The general objectives of the Mir Photo/TV Survey are as follows:

- Provide assurance of crew and Orbiter safety while in the proximity of the Mir Station.
- Assess the overall condition of the Mir.
- Study the effects of the space environment on a long-duration orbiting platform.
- Understand the impact of plume impingement during proximity operations.
- Evaluate the equipment and procedures used to gather survey data.

STS-71 provided an opportunity to survey areas of the Mir station that were not visible during STS-63. Detailed imagery of the Orbiter-facing sides of the Kvant-2 and Spektr modules, along with the forward facing-side of the Kristall module, were acquired for the first time. Good overview imagery of the other modules and arrays was also obtained. In terms of motion analysis, since braking pulses were not required during the final feet of approach, no Mir solar array motion was seen that could be attributed to Shuttle thruster firings. However, analysis was performed on two separate sequences of approach video data where the Base Block arrays were seen to oscillate. Procedures used for the different analyses are described in their respective sections. The following tasks were based on user requirements:

- Verify the configuration of the Mir complex.
- Assess the effect of micro-meteoroid impacts on Mir surfaces.
- Document the condition of the docking mechanism.

- Analyze the effect of Shuttle and Mir RCS thruster firings on the Mir complex during approach and backaway.
- Determine the usefulness of imagery data in calculating approach and backaway velocities.
- Characterize the motion of Mir appendages during the Shuttle Primary Reaction Control System (PRCS) test.
- Compare image quality of the Electronic Still Camera (ESC) to the Nikon camera.
- Assess the quality of video and photographic data.

1.2 Summary of Findings

A summary of findings from each of the aforementioned analysis tasks follows.

1.2.1 Mir Configuration

Configuration information is important for proximity operations requiring visual navigation and for conducting loads simulations of docked configurations. Documentation of the Mir station was compared to photography acquired during the rendezvous. The fly-around view shown in Figure 1-A identifies different Mir modules photographed during STS-71.

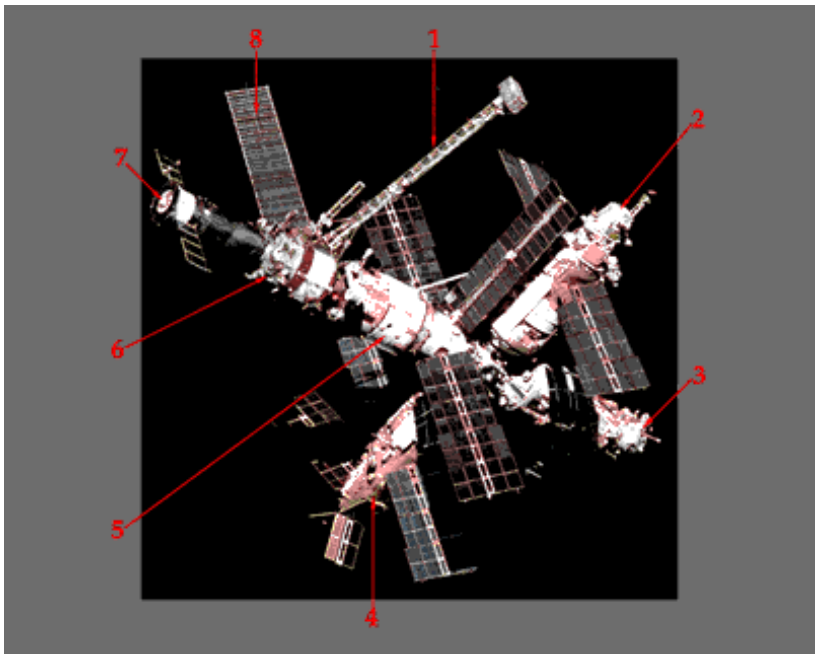

Figure 1-A Fly-around View of Mir Station

1. Sofora Truss
2. Kvant II
3. Kristall
4. Spektr
5. Base Block
6. Kvant
7. Soyuz
8. Kvant Array (moved from Kristall)

1.2.2 Mir Survey Coverage and Surface Assessment

A Mir surface assessment was performed to study the effects of the space environment on station materials. Several minor surface impacts were noted on the radiators of the Kvant-2 module. Two tears to the thermal insulation on the Kristall module were noted. As expected, detailed photography of the new Spektr module did not reveal micrometeoroid impacts. Other visible damage included several locations where individual cells on the Kvant solar array appeared to be peeling away from the backing material. Also, areas of discoloration were noted on the Mir Base Block and around different antennae. Figures 1-B and 1-C document the extent of detailed and overview (i.e., video and/or fly-around still photography) coverage of the Mir Station acquired during STS-71.

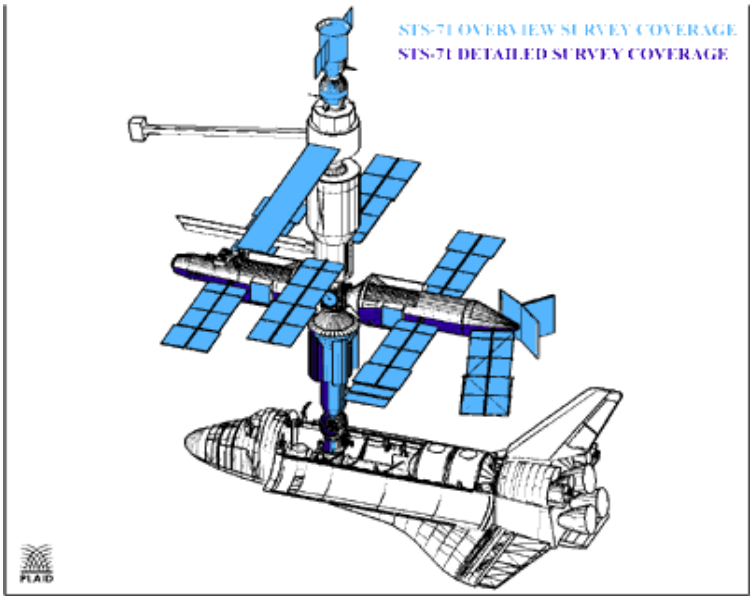

Figure 1-B STS-71 Mir Survey Coverage (Top View)

Note that none of the solar arrays are classified as having been covered in detail. This is primarily due to the fact that limited detailed coverage of the solar arrays has been obtained due to panel orientation, lighting conditions and crew time constraints. However, Orbiter-facing sides of the Kvant-2 and Spektr modules were imaged in detail on this mission.

STS-63 survey coverage, along with the cumulative Mir survey coverage status, is displayed in Appendix B.

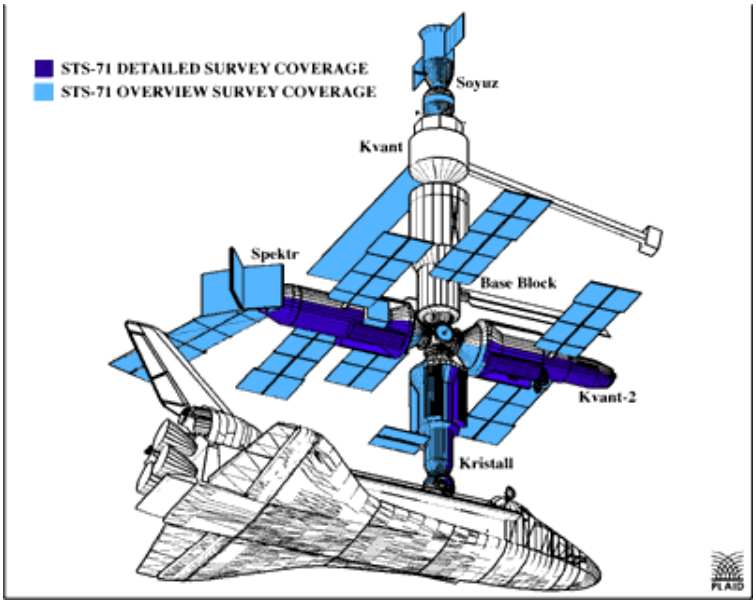

Figure 1-C STS-71 Mir Survey Coverage (Bottom View)

1.2.3 Docking Mechanism Assessment

The Payload Integration and Engineering Office (MS2) is assessing the condition of the Kristall docking mechanism. The old docking target backplate installed prior to STS-63 was replaced during STS-71. Both video footage and photographic data were acquired of the docking mechanism and target during the rendezvous. In general, the targets and surrounding area appeared to be free of damage and in good condition. Additionally, a systematic photographic survey of the returned target was performed on the ground to assess the effect of the space environment.

1.2.4 Solar Array Motion

Concerns about clearances during docking operations was the motivation for attempting to detect plume impingement. Since braking maneuvers were unnecessary during the final approach phase, no Shuttle plume impingement data was collected at that time. However, Base Block solar array motion was noted on two different occasions while the Mir was maneuvering into docking orientation. No conclusive determination can be made from the data, but both of these events may be related to Mir thruster firings.

1.2.5 Primary Reaction Control System Test Video Analysis

The Structures and Dynamics Branch (ES2) performed tests to determine the effect of firing the Shuttle Primary Reaction Control System (PRCS) jets on the Mir structure. Video data of the Spektr, Base Block, and Kvant arrays was acquired, and motion and frequency analyses were performed on each test firing. The results of this effort can be correlated with accelerometer data gathered from the Mir station.

1.2.6 Motion Analysis from Video

The Image Science & Analysis Group (SN5) is continuing to evaluate the use of payload bay camera video data to measure motion. During approach and backaway procedures, the Trajectory Control System (TCS) was used to determine distances from the Orbiter to the Mir station. As on STS-63, the trajectory data was compared to calculations made from photogrammetric analysis of video data. This comparison will help future motion analyses when only imagery sources are available.

1.2.7 Imagery Evaluation

The STS-71 image data and acquisition procedures were evaluated. This mission marked the first time that the Electronic Still Camera (ESC) was available for DTO-1118 image acquisition. ESC imagery is unique in that it allows capture and transmission of digital imagery that is of higher resolution than video. No quantitative comparison of ESC and Nikon imagery was performed due to variation in lighting conditions and time of acquisition. Representative views of identical scenes are shown for subjective comparison. Assessment of this data is being performed to identify problems with procedures and equipment for subsequent rendezvous missions.

2. MIR CONFIGURATION

A detailed assessment of the STS-71 configuration is presented. This involved identifying and labeling features directly from the photography. A comparison of expected and actual station elements revealed features that were not identified in the documentation. These features are labeled as 'unknown' in the following images and will be discussed with Russian investigators.

Figure 2 shows the station as it appeared during the STS-71 approach. The digital composite image seen in Figure 2 was constructed from NASA photographs STS071-701-005 and STS071-701-007.

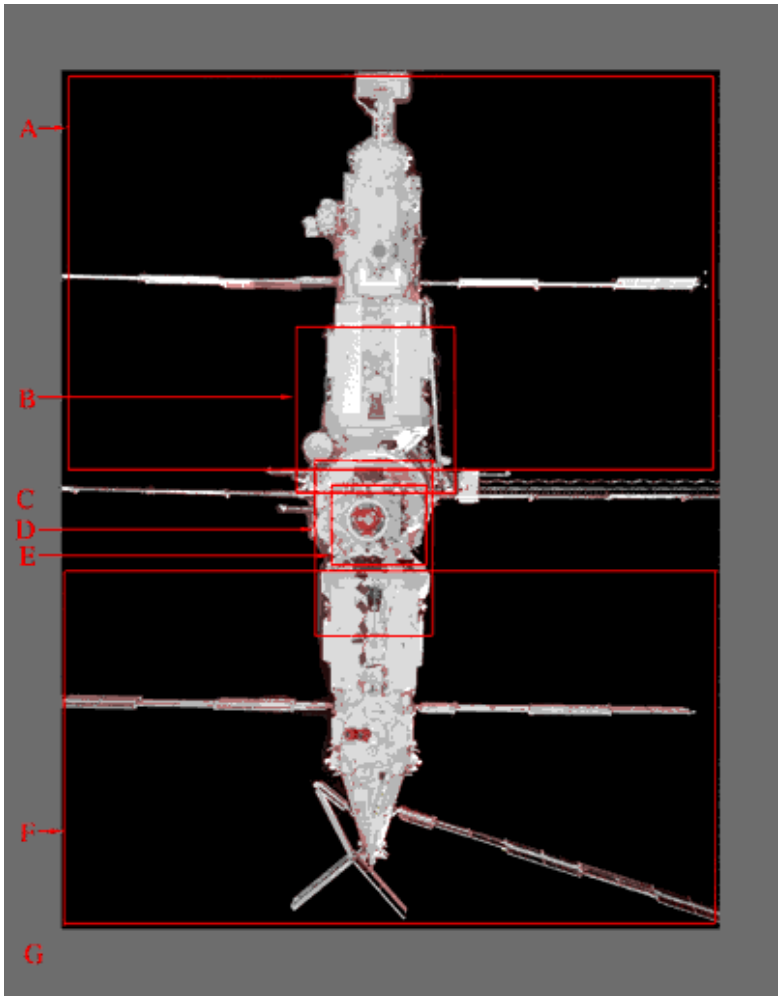

Figure 2 Mir Station during Approach (Mosaic View)

The boxes labeled A - G encompass regions whose exterior surfaces are described in detail within this section. Boxes C and G are regions which are not observable in this view. Kvant-2 (A and B) was the second module to dock with the Mir base block. It's primary purpose is to support extravehicular and remote sensing activities. Part of box B and all of

C refers to the Kristall module. This module is used for material processing, remote sensing, and vehicle docking. The docking module (D and E) has two androgynous peripheral docking units (E). Box F identifies the Spektr module. This module is the latest addition to the Mir station. It's primary objective is to study the environment and the earth's atmosphere. Box G refers to the Soyuz TM. The Soyuz capsule is used to transport cosmonauts and astronauts between Mir and earth. During STS-71, Soyuz was used to document the undocking of the Shuttle from the Mir.

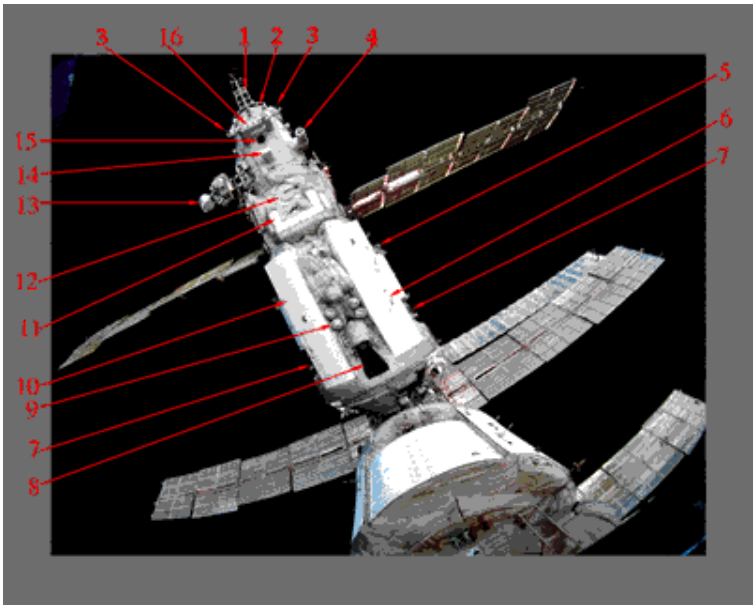

Figure 2-A Kvant-2

1. **Materials Exposure Platform**
2. **EVA Hatch**
3. **Attitude Control Engines**
4. **"Phase" Spectrophotometer**
5. **Tether Attach Fixture**
6. **Antenna**
7. **Attitude Control Engines**
8. **Maneuvering and Approach Engine**
9. **Infrared Device for Orientation to Earth**
10. **Propellant Tanks (under Radiators)**
11. **Gyrodine Case**
12. **Window**
13. **TV Camera**
14. **Scientific Instrument**
15. **Window**
16. **Infrared Device of Orientation**

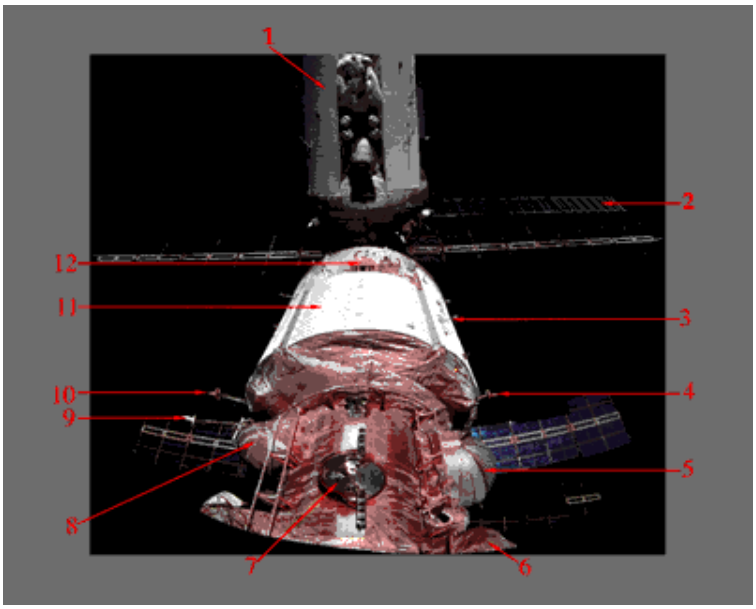

Figure 2-B Kristall and Kvant-2

1. **Kvant-2 Module**
2. **Kvant Array**
3. **Antenna**
4. **Igla Antenna**
5. **Glaser Telescope**
6. **“Ksenia” Device**
7. **Solar Array Attach Point**
8. **“Rodnic” Water Tank**
9. **Command Radio Link Antenna**
10. **Igla Antenna**
11. **Kristall Module**
12. **Attitude Control Thrusters**

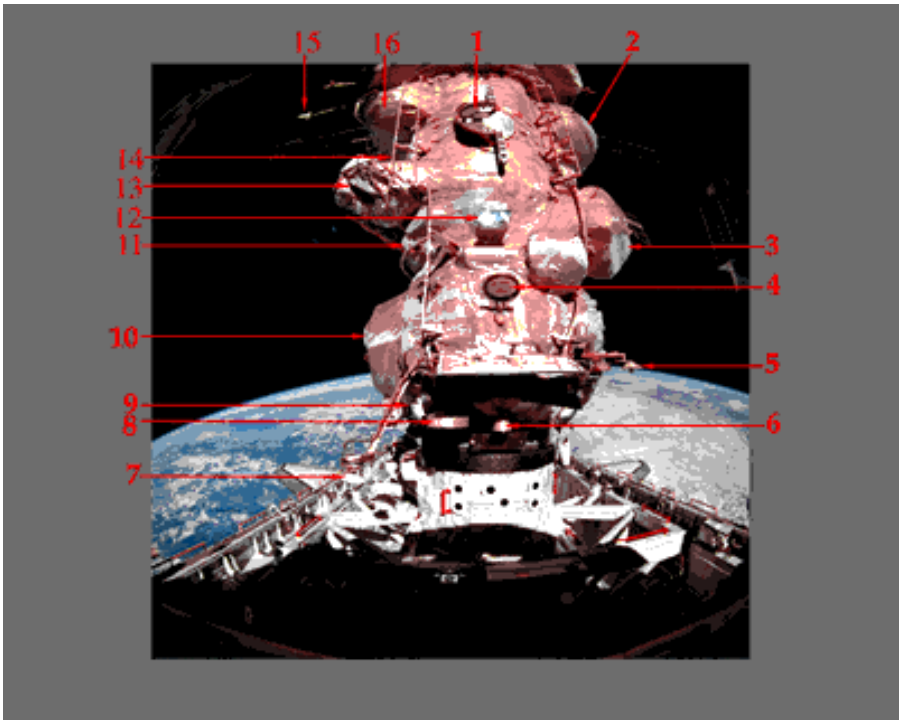

Figure 2-C Kristall and Orbiter Payload Bay

1. **Solar Array Attach Point**
2. **Glaser Telescope**
3. **“Ksenia” Device**
4. **Window**
5. **“Kurs” Docking System Parabolic Antenna**
6. **Mooring and Stabilization Engines**
7. **“Kurs” Docking System Parabolic Antenna**
8. **Buran TV Target**
9. **Sun Sensor**
10. **Photo Compartment**
11. **Circular Handrail**
12. **Container Attach Fixture**
13. **Container with Gearing of Solar Array**
14. **EVA Handrails**
15. **Command Radio Line Antenna**
16. **“Rodnic” Water Tank**

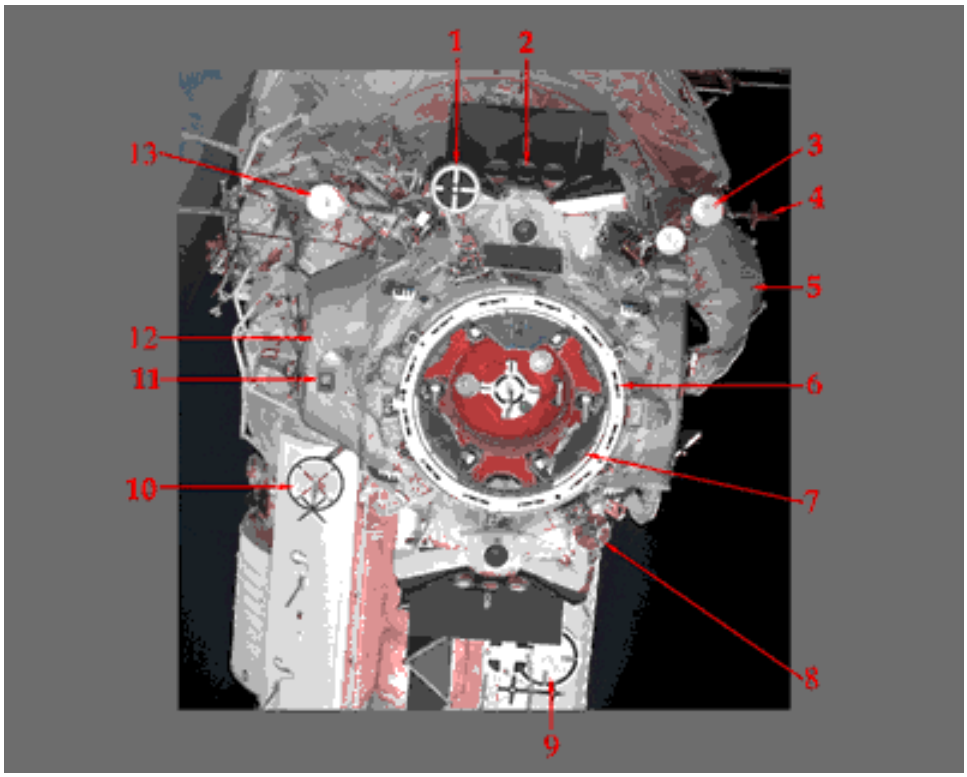

Figure 2-D Docking Mechanism during Approach

1. **Buran TV Target**
2. **Mooring and Stabilization Engines**
3. **“Kurs” Docking System Parabolic Antenna**
4. **Igla Antenna**
5. **“Marina” Apparatus**
6. **Structural Latch**
7. **Capture Latch**
8. **Igla Antenna**
9. **Target for Docking and Stationkeeping**
10. **Soyuz TM Target**
11. **Video Camera**
12. **Photo Compartment**
13. **“Kurs” Docking System Parabolic Antenna**

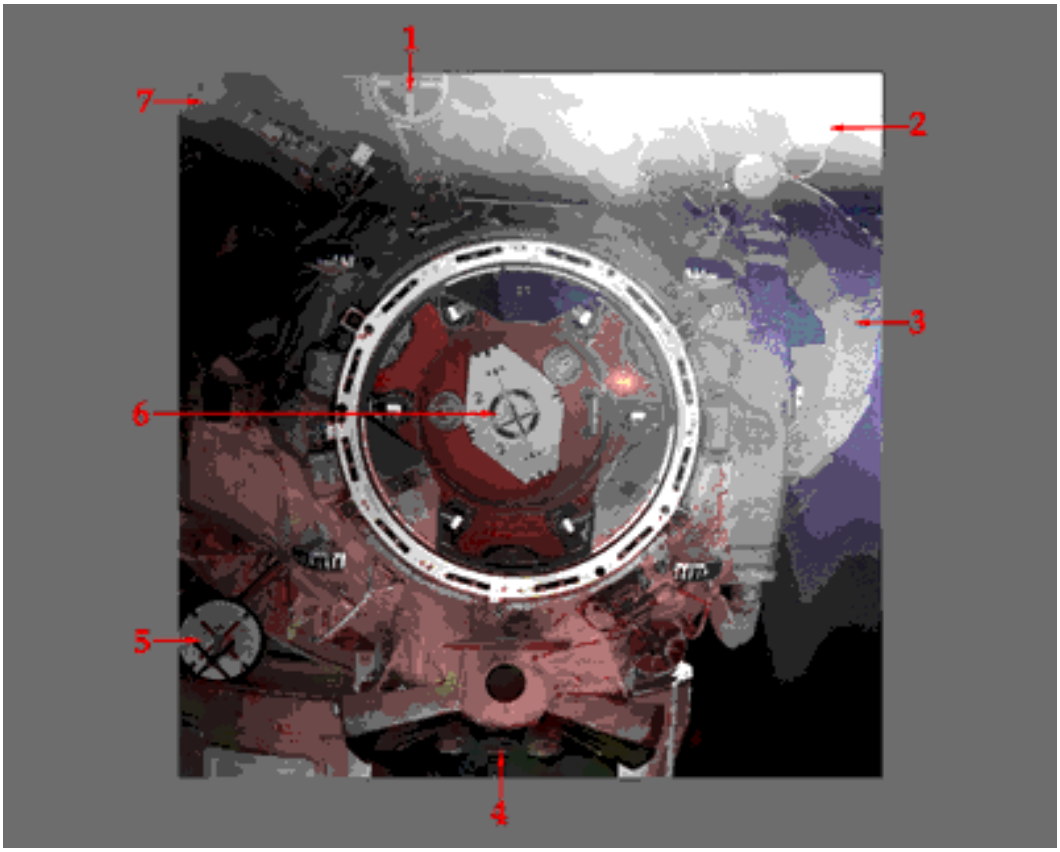

Figure 2-E Docking Mechanism during Backaway

1. **Buran TV Target**
2. **“Kurs” Docking System Parabolic Antenna**
3. **“Marina” Apparatus**
4. **Mooring and Stabilization Engines**
5. **Soyuz TM Target**
6. **New Centerline Docking Target**
7. **“Kurs” Docking System Parabolic Antenna**

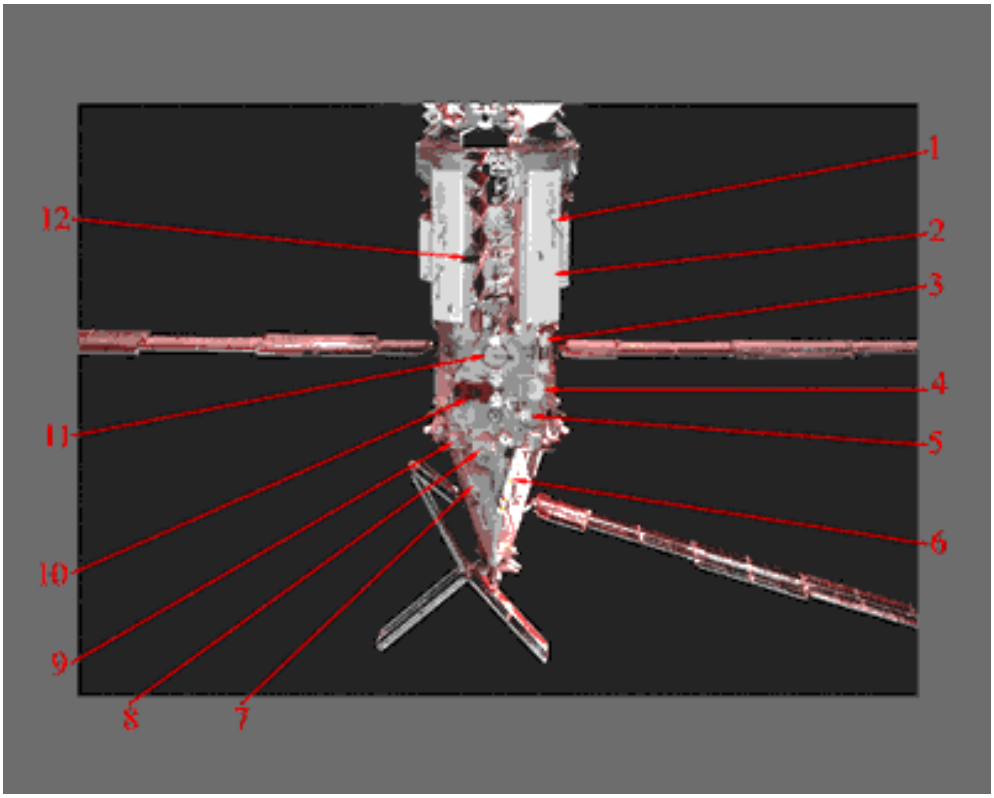

Figure 2-F Spektr Module

1. **Antenna on External Cooling Radiator Panel**
2. **Radiator**
3. **Standardized Landing Panel**
4. **Scientific Airlock**
5. **Nest**
6. **European Science Exposure Facility**
7. **BRIZ Instrument**
8. **Phoenix Instrument**
9. **Scientific Instrument**
10. **Payload Pointing System**
11. **Viewport**
12. **Kristall Solar Array**

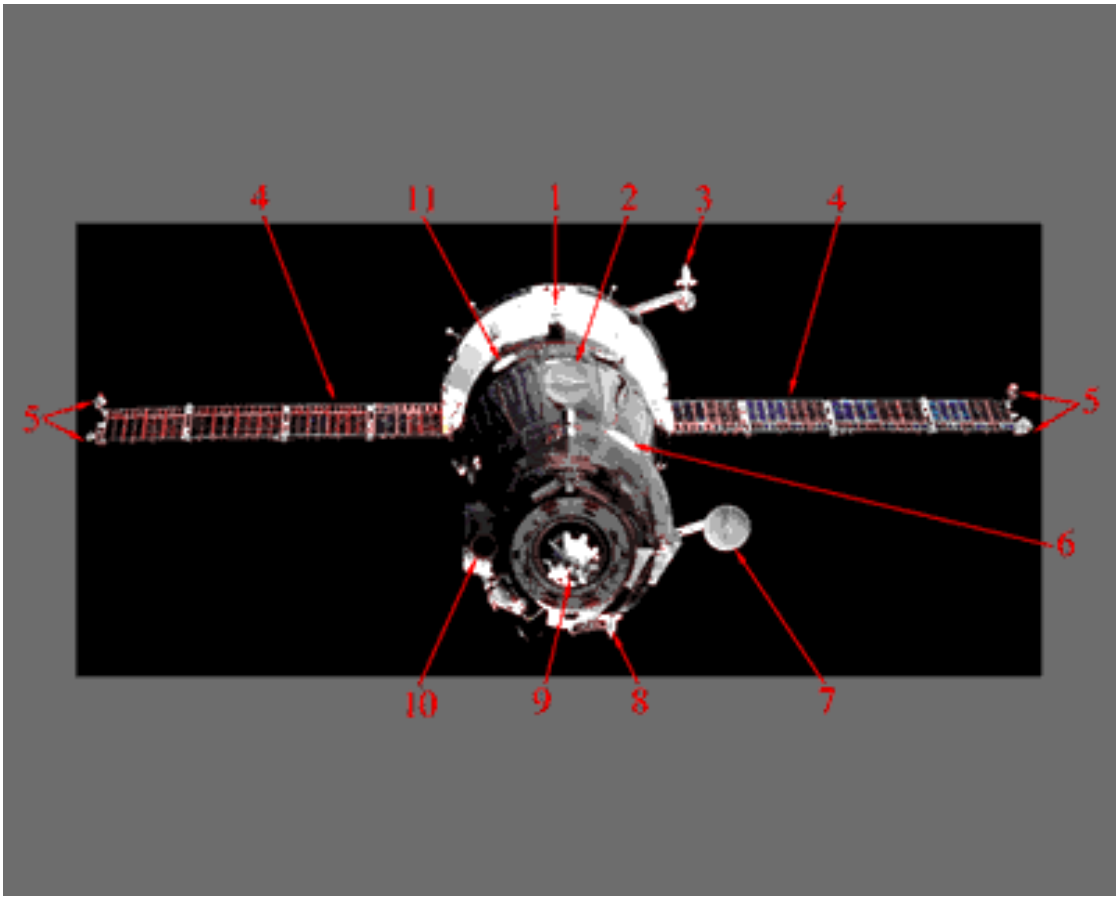

Figure 2-G Soyuz Capsule

1. **Sun Sensor**
2. **Approach System Auto Tracking Antenna**
3. **Approach System Omni-directional Antenna**
4. **Solar Array**
5. **Antennae**
6. **Side Hatch**
7. **Approach System High-gain Antenna**
8. **Approach System Pointing Antenna**
9. **Docking Unit**
10. **Blister Window**
11. **Command Radiolink Antenna**

3. MIR SURVEY COVERAGE AND SURFACE ASSESSMENT

A survey of the visible Mir station components was performed to identify areas of damage and discoloration. Measurements of this damage were obtained where possible using photogrammetric procedures on digitally scanned images. A tabular list of visible damage and discoloration is located in Appendix A. In addition, this list identifies those areas previously seen during the STS-63 survey.

Figure 3-A is an overview image of the Mir Space Station taken during the fly-around phase of the rendezvous. This image provides a complementary overview to the data collected on STS-63. The side of the Mir Base Block seen in this view is opposite to that seen on STS-63 imagery.

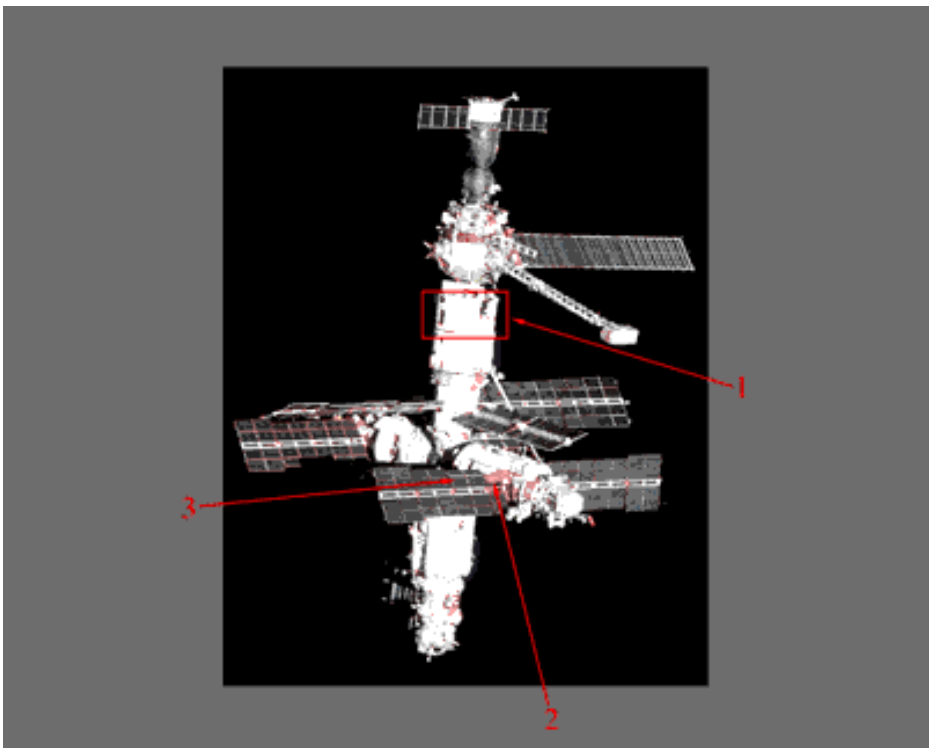

Figure 3-A Overview Fly-around View

Item 1 identifies the upper section of the Mir Base Block where discoloration is observable. This discoloration appears to follow along the seams of adjacent panels. Similar observations were made on STS-63 for the opposite side of the Base Block.

Items 2 and 3 identify damaged panel sections of a Kvant-2 solar array. The panel labeled 2 has been folded backwards upon itself. Item 3 refers to the adjacent panels that are bowed in the opposite direction.

The Kvant-2 module was hidden from view on STS-63. During the docked phase of STS-71, the module was located directly above the Shuttle flight deck. This provided an opportunity to gather baseline surface assessment information. Figure 3-B shows the upper airlock section of the Kvant-2 module.

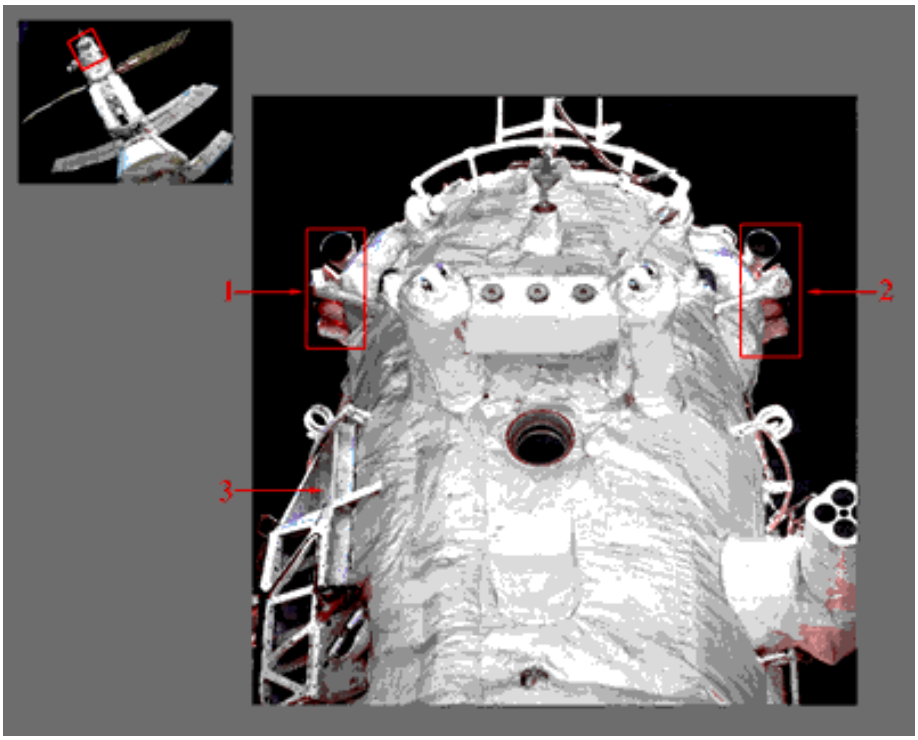

Figure 3-B Kvant-2 Thrusters and Support Structure

Items 1 and 2 identify areas around the attitude control engines. All the visible nozzles with this configuration on the Kvant-2 module seem to show some degree of discoloration. Russian investigators have attributed this type of discoloration to propellant residue. The identification of these areas will help in the analysis of plume dynamics on the International Space Station.

Item 3 identifies a discolored support structure. Some of the blankets covering large surfaces displayed spots and/or blotchy patterns. Discoloration observed on this blanket appeared to be concentrated in an area near the structural interface.

Figure 3-C shows the lower portion of the Kvant -2 airlock section. Two observation ports are visible. The observation port window cover at the top is in a closed position.

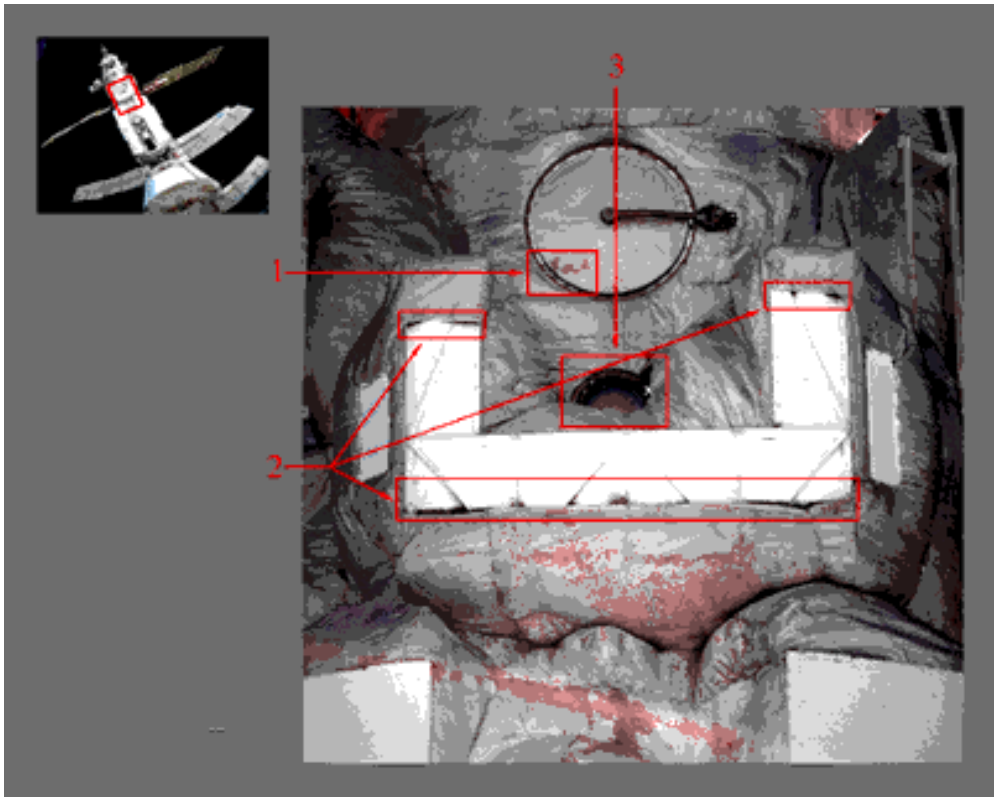

Figure 3-C Kvant-2 Airlock Section

Item 1 identifies an area of discoloration on the observation port cover.

The arrows in item 2 point to areas of discoloration located near the interface region between the surface structure and blanket material.

Item 3 identifies an observation port window partially blocked by a blanket. This may be due to loose folds in the material that have propagated since the original deployment.

Figure 3-D exhibits the blanketed area between the radiators on the Kvant-2 Module.

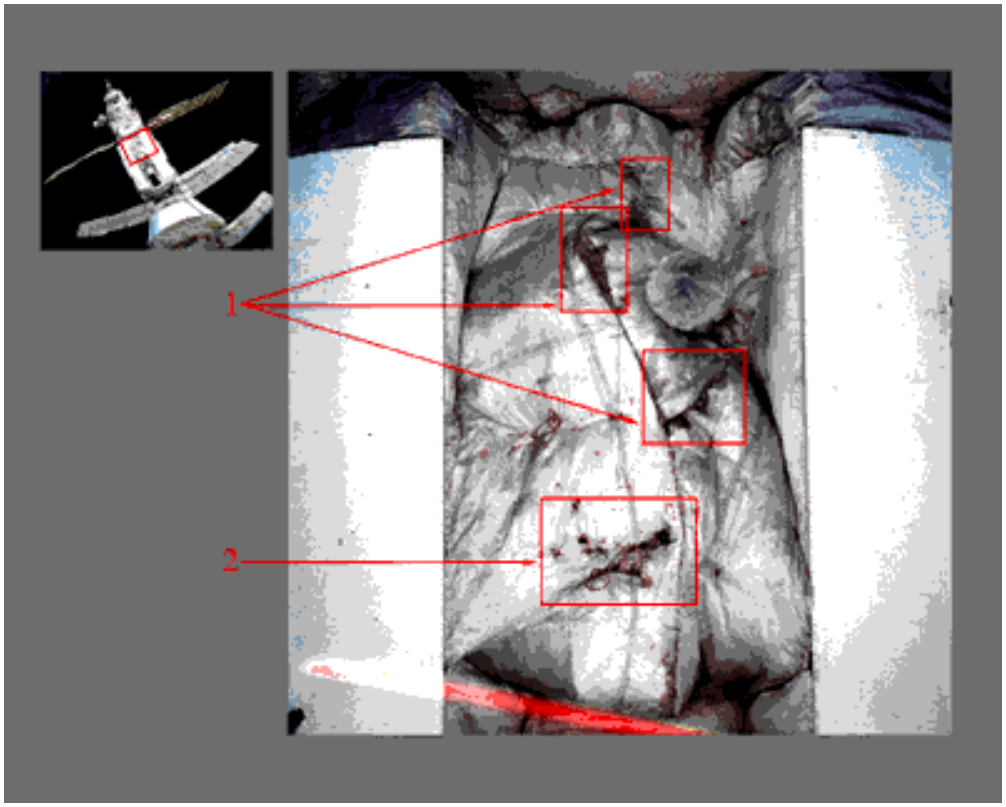

Figure 3-D Kvant-2 Blanketed Area between Radiators

Item 1 exhibits discolored areas on the blanketed area between the radiators.

Item 2 identifies possible blanket damage. The particular areas of interest seem to reveal some underlying structure(s). This indicates holes or openings that are evident in the blanket.

Some of the areas of greatest concern to Russian investigators are the radiator panels on the station. Anomalies are hard to detect on these surfaces because exposure settings tend to wash out blemishes on a pure white background. On this mission, however, several excellent images of radiator surfaces revealed possible impact locations.

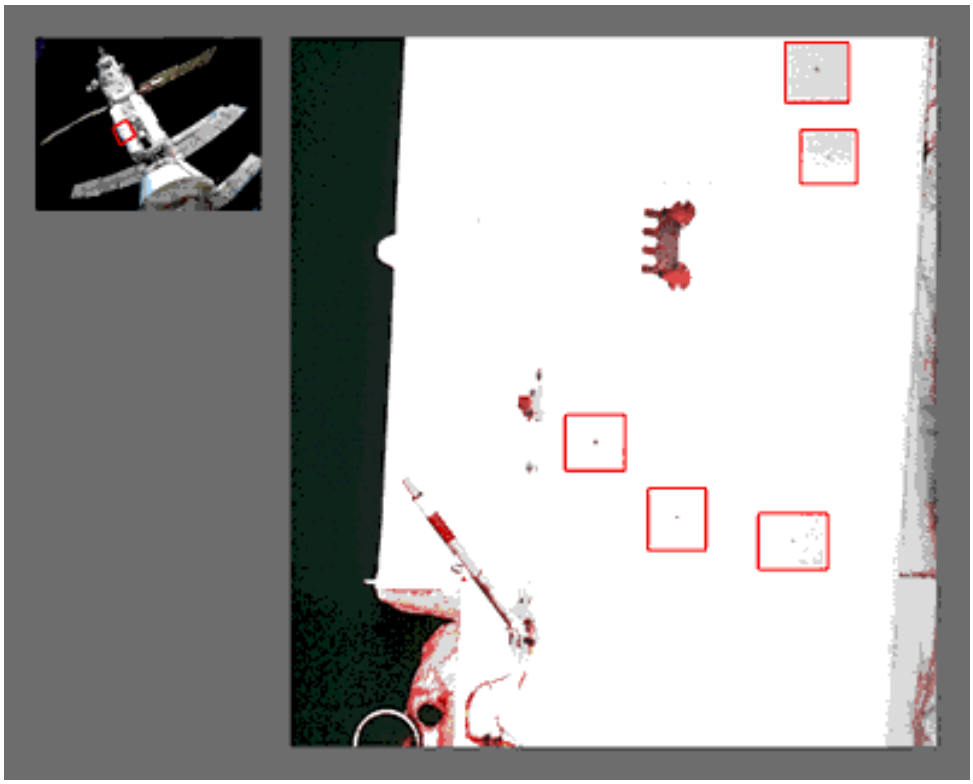

Figure 3-E Possible Impacts to Kvant-2 Radiator

At least five potential impact points were identified on this radiator panel. These impacts did not exhibit symmetric or linear pattern distributions associated with bolts and/or rivets. In addition, the points appeared to be reddish in color. This is inconsistent with other observed bolts and rivets. Regions outlined in red on the image have been enhanced to show possible micrometeoroid impacts. The diameters of these impacts are on the order of 1 cm.

Figure 3-F is an image of the endcone on the Kvant-2 module. This particular section of the module interfaces with the multi-docking node. The silver and white feature seen at the top right corner of the image is the Ljappa arm. This arm is used to reposition modules to different nodes on the Station.

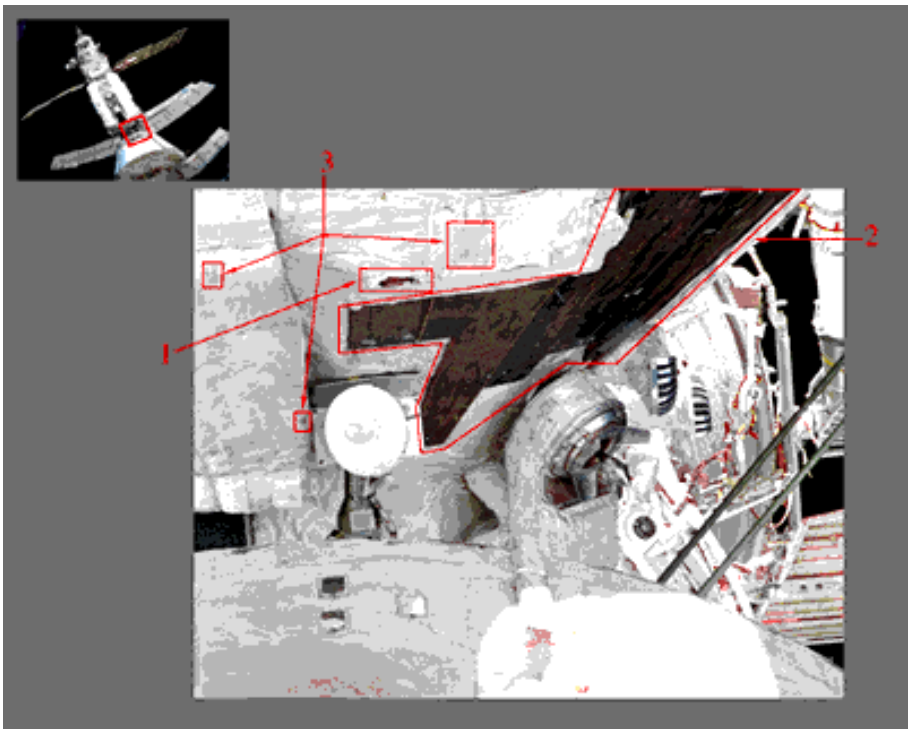

Figure 3-F Kvant-2 Conical Section

Item 1 identifies a section of blanket which appears to be torn. The length of this tear was measured to be 12 cm.

Item 2 highlights an area on the Kvant-2 endcone. A determination has not yet been made as to whether the region is actually missing thermal protection or is intentionally kept clear. The approximate area of this feature is 1460 cm^2.

Figure 3-G shows an expanded view of the junction between the Kvant-2 (top) and Kristall (bottom) modules. From this perspective, the Base Block and Kvant solar arrays can also be seen in the background.

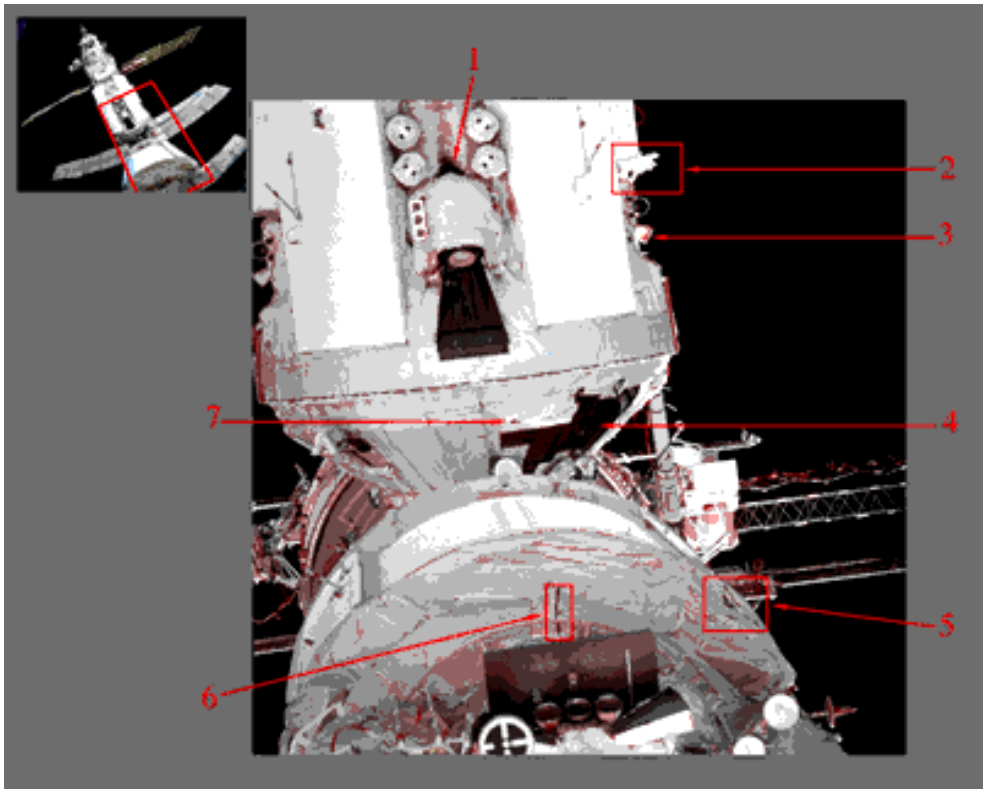

Figure 3-G Expanded View of Kristall / Kvant-2

Item 1 is a dark discoloration in the crevasse behind the positioning and docking engines on the Kvant-2 module. Closer scrutiny of this area during the ground-controlled video survey indicated that the discoloration was not due to shadowing.

Item 2 shows possible frayed blanket material near the attitude control engines.

Item 3 identifies discoloration on the attitude control engines.

Item 4 points to the barren area observed on the conical section of the Kvant-2 module (discussed in Figure 3-F).

Item 5 identifies four tears in the thermal blankets adjacent to the Kristall radiators. The length of these tears range from 9 cm to 27 cm. On STS-63, only one tear was distinguishable. A close-up view of two of these tears is shown in Figure 3-I.

A dark linear feature near a Kristall solar array attach point is identified as item 6. A determination has not been made on whether this feature is an anomaly.
Item 7 identifies a section of detached blanket material (also seen on Figure 3-F.)

Figure 3-H is a close-up view of the attitude control engines near the top of the Kristall module. This area is also close to the junction between Kristall and Kvant-2.

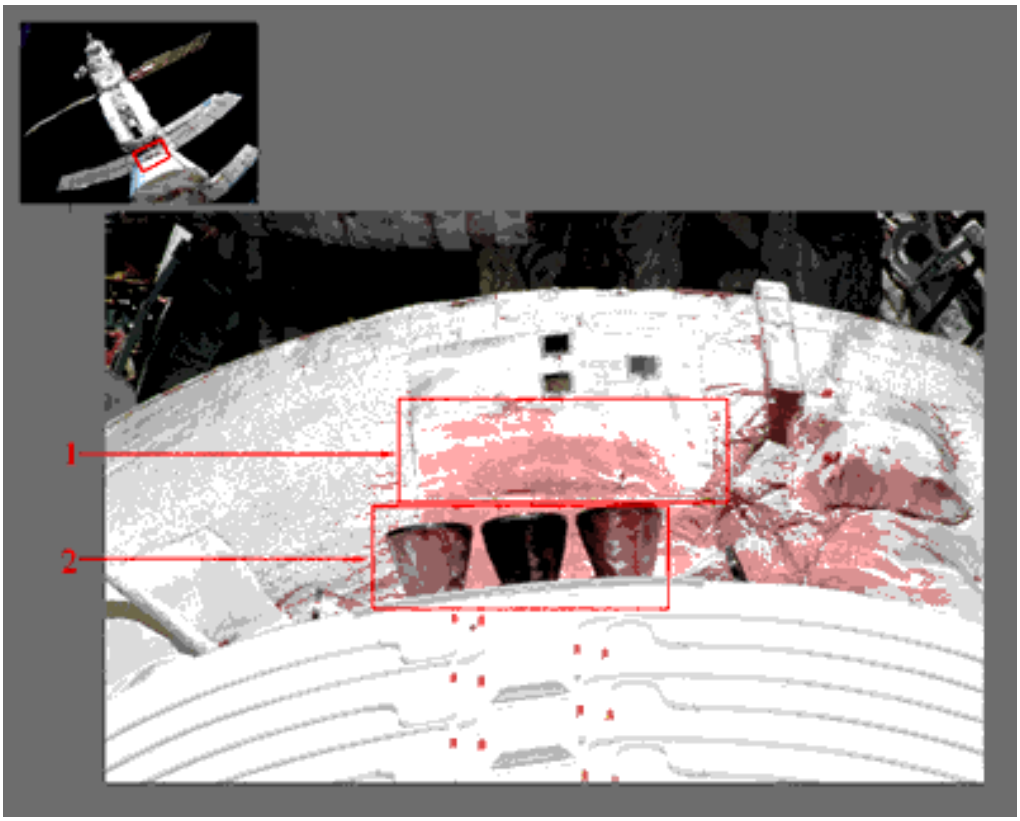

Figure 3-H Upper Kristall Thrusters

Item 1 points out discoloration on the blanketed area above the attitude control engines. Scattered white dots can also be seen in this region. Investigators have attributed this type of discoloration to propellant residue.

Item 2 identifies possible dents on the attitude control engine nozzle covers. In addition, this view shows discoloration to the nozzle area.

Figure 3-I provides a close-up view of the torn blanket observed on the Kristall module (referred to in Figure 3-G). The Kurs antenna located on the Kristall module is also visible in this view.

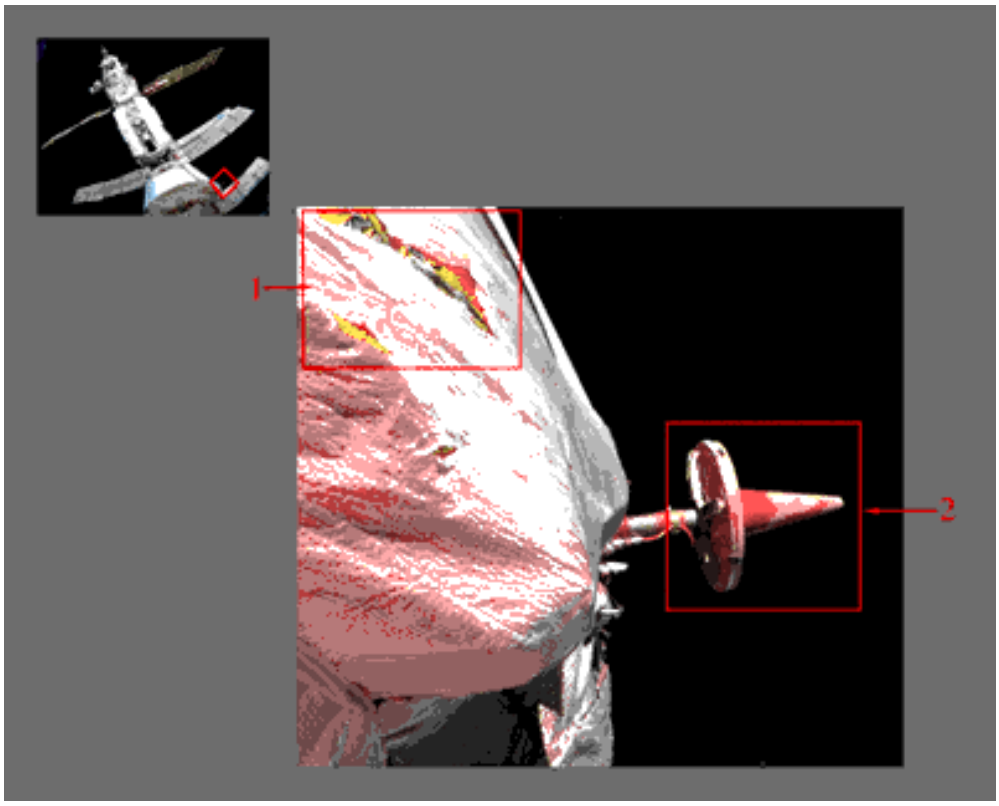

Figure 3-I Close-up of Kristall Module and Kurs Antenna

Item 1 is a view of two tears on the thermal protection blanket area adjacent to the Kristall radiators. These tears were measured to be 17 cm and 9 cm in length. Additional measurements of adjacent tears are noted in Appendix A.

Item 2 highlights discoloration of the Kurs antenna. Possible sources for the cause of this discoloration are propellant residue or degradation due to atomic oxygen.

Figure 3-J is the forward facing side (relative to the Shuttle cargo bay) of the docking module on Kristall. The rectangular-shaped object near the center of the image is the blast deflection plate for the mooring and stabilization engines.

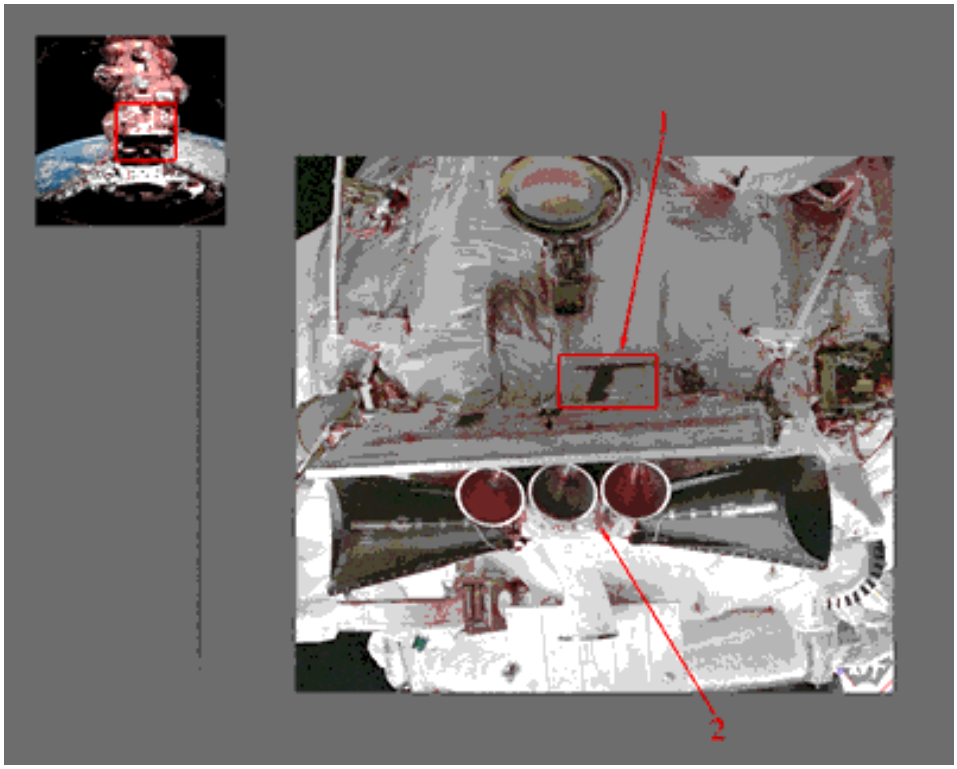

Figure 3-J Lower Kristall Thrusters

Item 1 points to a dark discoloration on the blanket material above the blast deflection plate. Russian investigators will be contacted to determine whether this could be a result of leaking propellant.

Item 2 points to another area of discoloration beneath the mooring and stabilization engines.

Figure 3-K shows a close-up view of the Spektr Module. This module is the most recent addition to the Mir Space Station. As such, it provides an excellent opportunity to analyze the effects of the space environment on a brand new platform. As expected, Spektr surfaces appeared clean and damage free.

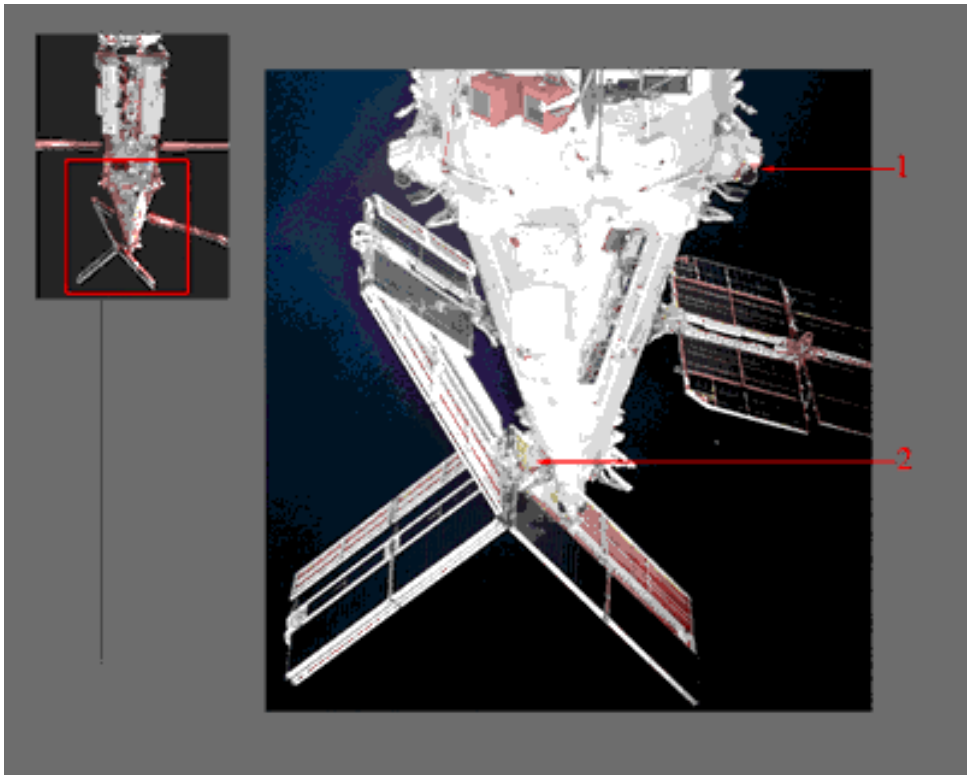

Figure 3-K Spektr Nose Cone

Item 1 identifies slight discoloration on the attitude controls engines. According to Russian investigators, this type of discoloration is common for engine nozzles and surrounding areas.

A restraining bolt inhibited proper deployment of one Spektr solar array. Item 2 shows the array as it was seen during STS-71. Image survey data of this area gathered during the mission was forwarded to the Russians. This array has since been repaired during an EVA by the Mir-19 crew.

Figure 3-L shows a view of the Kvant (top) and Base Block (bottom) solar arrays. The array on the Kvant module was previously located on the Kristall module. The array was moved as part of the Mir reconfiguration between STS-63 and STS-71.

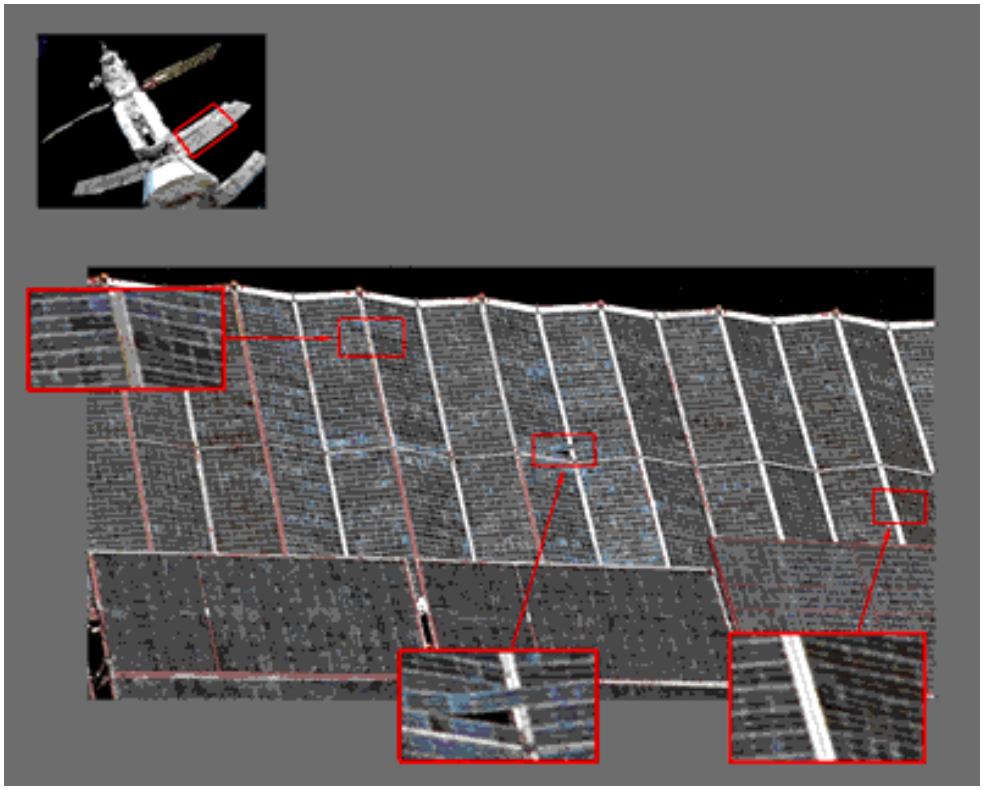

Figure 3-L Kvant Solar Array

Item 1 identifies three prominent areas where solar cells are seen detaching from the Kvant array. Six such areas of cell detachment were located and another 20 instances of loosely attached cells or possible damage were noted. This anomaly has not been seen on the other Mir arrays (such as those on the Base Block or Kvant-2.)

4. DOCKING MECHANISM ASSESSMENT

A target viewing assessment was performed to evaluate the performance of the primary video camera (ODS centerline) used during the approach and backaway. This imagery is referenced to payload bay camera 'C' footage as well as the best available still photography acquired from the Hasselblad 70 mm film camera.

Also, a detailed photographic survey of the old docking target was performed upon mission completion. Several minor impacts (possibly due to orbital debris) and some discoloration to the old target were noted and are documented in Appendix D.

4.1 Docking Target Condition

Hasselblad (70 mm) photography provided the best views of the APDU. The docking structural latches, capture latches, body-mounted latches, alignment guides, laser retroreflectors, fluid/electrical socket/plugs, and the old centerline target all appeared to be in good condition. Imagery acquired during backaway verified that the new centerline target was also in good condition.

4.2 Target Visibility Comparison

Figures 4-A, 4-B and 4-C on the following page document views taken of the target from the ODS centerline camera, payload bay camera 'C' and the Hasselblad during approach. All three images were taken during the approach phase. The still photograph was taken about a minute after the two video views.

Since the primary function of the ODS centerline camera was to provide the crew with a means to visually align the target during approach, a zoomed-out configuration was used to provide the widest field-of-view. Sun glare, visible on the bottom right corner of the image, severely hampered analysis during the latter stages of approach. From the image in Figure 4-A, one can verify the feathered configuration of the Mir arrays.

The crew also used payload bay camera 'C' to view the Mir during the final stages of approach. Figure 4-B shows that camera 'C' imagery was not adversely affected by sun glare during this time period. The zoomed in field-of-view easily allowed identification of targets and docking mechanism details from over a hundred feet away.

The still photograph in Figure 4-C was obtained using the Hasselblad camera with a 250 mm lens. Since the vantage point for image acquisition was the flight deck overhead window, sun glare similar to that seen on the upward pointing ODS centerline video was also a factor in the still photography. Most of the post-mission analysis of the docking mechanism was performed from this imagery.

Figure 4-A ODS Approach View

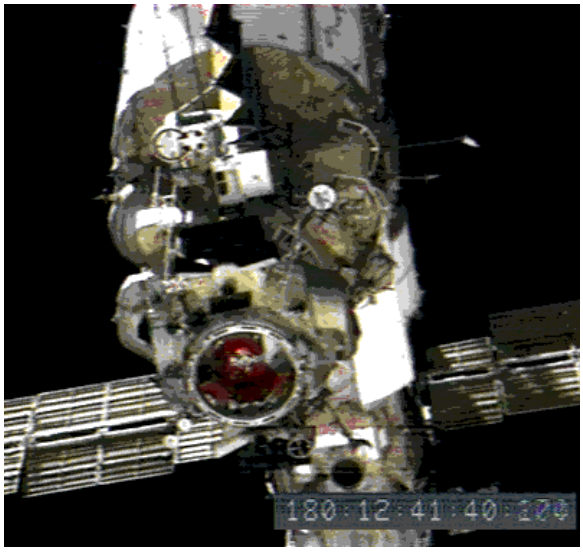

Figure 4-B PLB 'C' Approach View

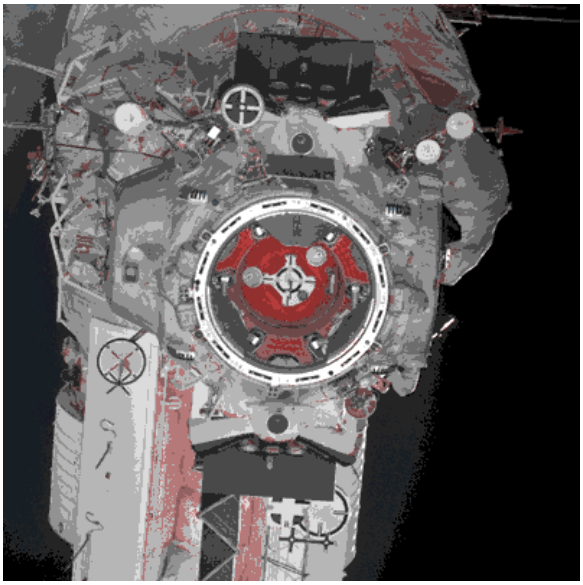

Figure 4-C Hasselblad Approach View

5. SOLAR ARRAY MOTION

5.1 Impingement Data

Data of Mir solar panel motion due to Shuttle RCS thruster plume impingement was to be gathered during the approach phase just prior to docking. Since no braking procedure was required, this data was not obtained. Additionally, views of the Mir solar panels could not be acquired during backaway because the sun was directly in the field-of-view.

5.2 Base Block Array Motion

Substantial motion of the Base Block solar arrays was visible during the early stages of approach as the Mir was changing orientation to prepare for docking operations. Figure 5-A shows the distance between the Mir and the Orbiter when the two different sequences of solar array motion were seen. Each pair of arrows refers to the start and stop times of observable motion.

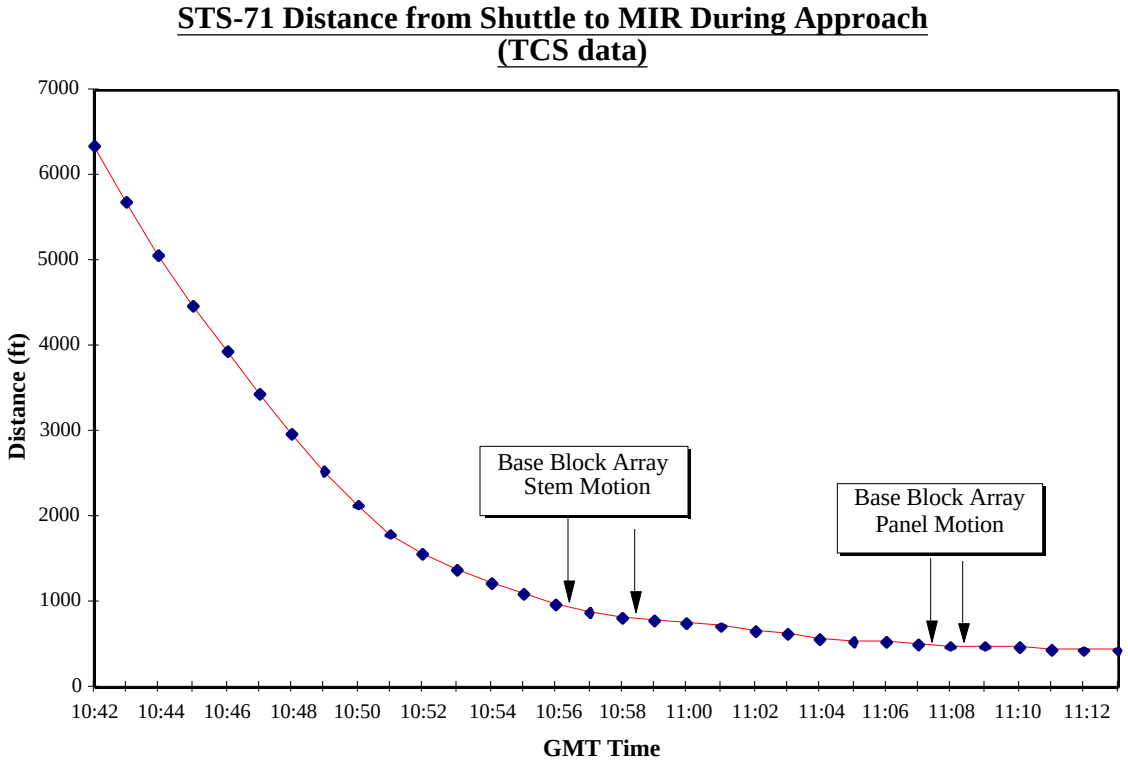

Figure 5-A Shuttle to Mir Distance During Stem / Panel Motion

5.2.1 Array Stem Motion

Base Block module thruster firings (in addition to those seen from thrusters at the end of the Sofora girder) were seen just as the Mir re-entered the payload bay camera 'B' field-of-view during approach. Significant motion of the Base Block (SP #1) array stem was seen during the next 90 seconds.

Figure 5-B depicts the payload bay camera 'B' field-of-view when the Mir solar array stem motion was visible. The procedure used to analyze the video data was as follows:

- Run an automated edge detection algorithm to track the motion of the Base Block array tip.
- Measure the amplitude of motion using features along the Base Block surface as a scaling factor. (Note that at a distance of ~1000 feet, the scale change between the array tip and the station surface is negligible.)
- Input the data into a one-dimensional Fast Fourier Transform (FFT) to isolate specific frequencies.
- Interpret the data to determine the existence of dominant frequencies.

Figure 5-B PLB Camera 'B' View Showing Base Block Stem Motion

Figure 5-C shows this motion as a function of GMT time. Figure 5-D plots the corresponding frequency of oscillation. Analysis of this motion indicated a maximum peak-to-peak magnitude of about 24 inches (+/- 20%) and a dominant frequency of 0.11 Hertz.

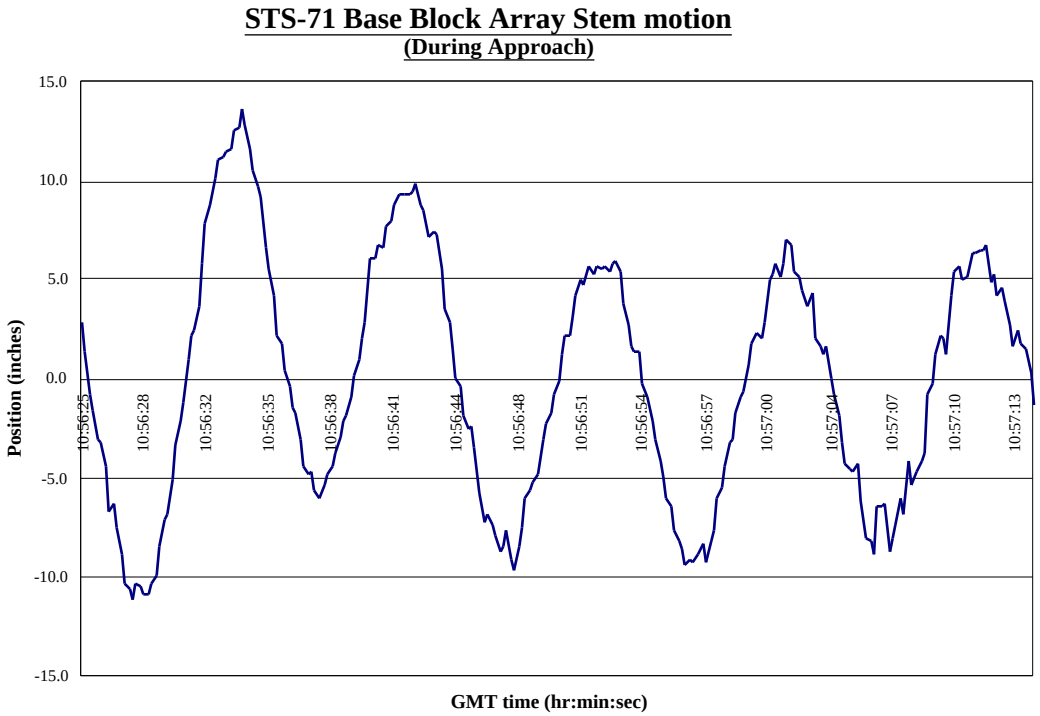

Figure 5 - C Base Block Array Stem Motion

STS-71 Base Block Stem Motion

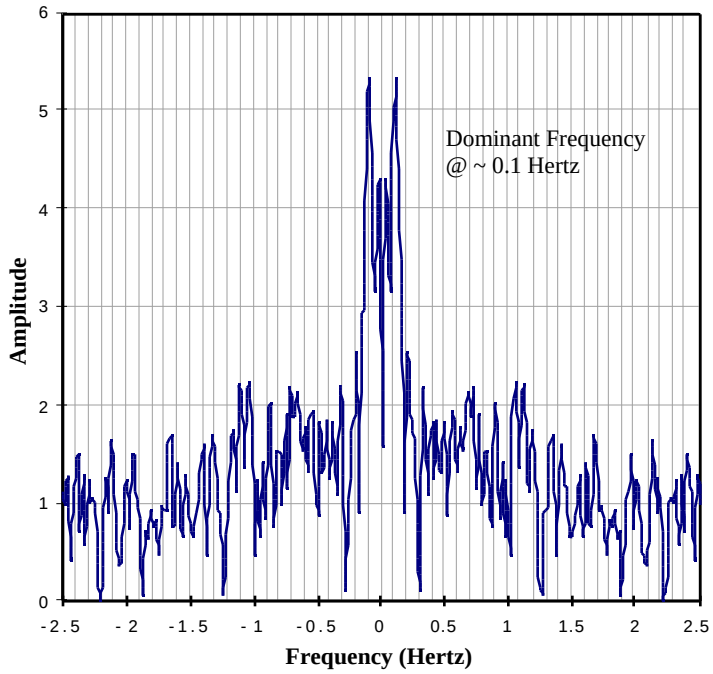

Figure 5-D Base Block Array Stem Motion Frequency

Analysis of this data suggests that the Mir Base Block solar panel stems and arrays are in a location such that attitude firings do impinge upon them. There are other factors that could have contributed to this motion. Start and stop forces induced by rotating panels may have contributed to the first visible motion sequence. Additionally, during the latter part of this time sequence, it appeared as though all the other arrays continued to rotate while those on the Base Block appeared to stop.

5.2.2 Array Solar Panel Motion

Motion of the lower panels on the opposite Base Block solar array (SP #2) was visible several minutes later. The payload bay camera 'B' scene appeared to shake slightly. Minor vibration of a payload bay camera field-of-view is usually indicative of a Shuttle Reaction Control System (RCS) thruster firing. An examination of Shuttle RCS data between 11:07:19 and 11:08:19 GMT suggested that pulses fired from the L2D/L3D and R2D/R3D thrusters appeared to coincide with this motion. Upon closer examination, however, array motion preceded the first of these pulses by about a second. This implied that a different source (possibly Mir thrusters hidden from the camera field-of-view) was the cause of this motion.

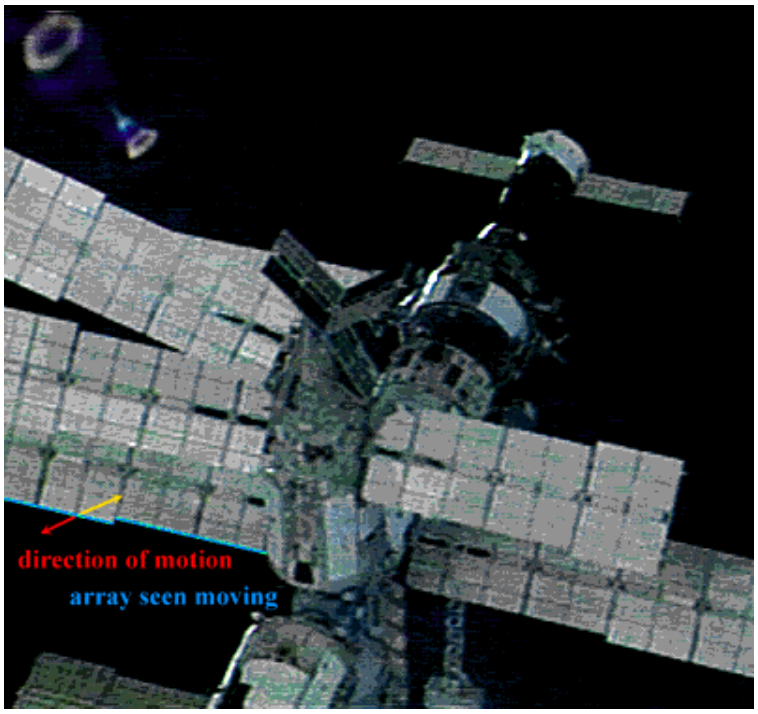

Figure 5-E PLB Camera 'B' View Showing Base Block Panel Motion

Figure 5-E depicts the payload bay camera 'B' field-of-view when the Base Block solar array panel motion was visible. The magnitude of this oscillation could not be measured due to the oblique camera angle relative to the direction of motion. However, a plot displaying frequency of the motion is shown in Figure 5-F.

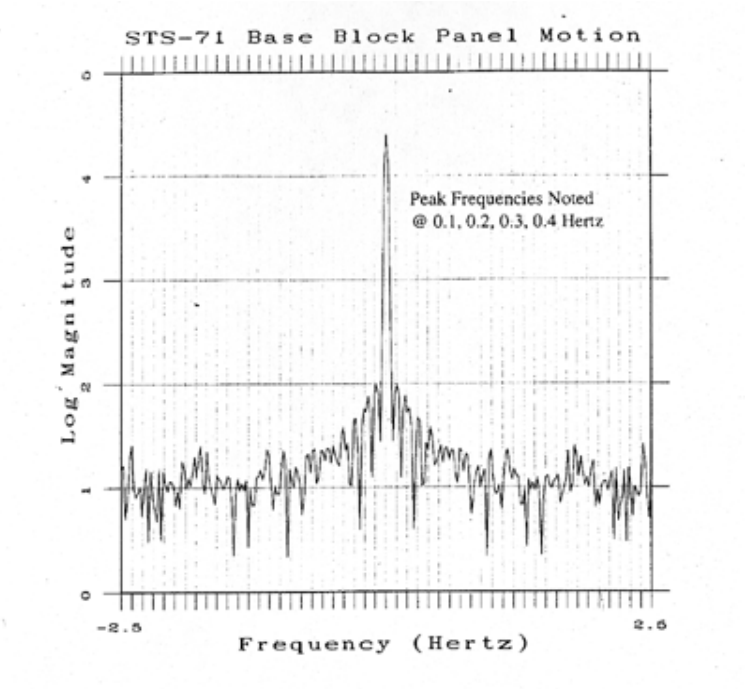

Figure 5-F Base Block Array Panel Motion Frequency

No dominant frequencies are apparent on the plot in Figure 5-F, although several minor peaks can be identified. The presence of these minor peaks at 0.2, 0.3 and 0.4 Hertz suggest that they may be harmonics associated with the peak at 0.1 Hertz.

In the first sequence, an entire solar array stem was in motion. During this second motion sequence, however, individual panels on the opposite Base Block array appeared to be moving in response to two specific pulses. Possible sources for this second array motion event seem harder to isolate. Video exposure levels and the rotating station hid the Base Block thrusters during this period of time. In addition, no clear views of the Base Block or Sofora thrusters were visible during this sequence. However, the nature of the motion - a response to two specific and separate pulses - would suggest Mir thruster firings as a possible source.

Results of this analysis have been forwarded to plume impingement specialists in the Structures and Dynamics Branch/ES2.

6. PRCS TEST VIDEO ANALYSIS

The Primary Reaction Control System (PRCS) test performed on STS-71 augmented accelerometer data gathered from Mir surfaces with video of structural appendages. The goal of this analysis was to determine the effect of using Orbiter thrusters to control Shuttle/Mir movement. Video data was used to determine maximum amplitude of motion of each of the three visible (Spektr SP #3, Base Block SP #1, and Kvant SP #1) arrays. In addition, analysis was performed to verify the presence of dominant frequencies in the array motion. Motion and frequency plots were generated from each of the eight specific tests documented in Table 6-A.

The procedure used in the analysis was similar to that used in the Base Block solar array motion calculations.

The accompanying image and plots are representative of the data and analysis performed. Complete plots of each test sequence are located in Appendix C.

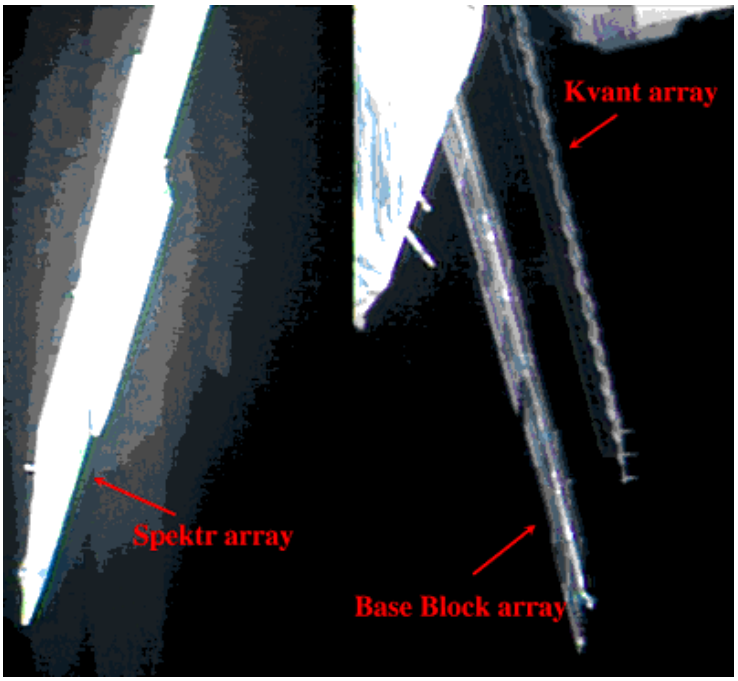

Figure 6-A Muxed Views of PRCS Test #7

A typical multiplexed view used in the analysis is shown in Figure 6-A.

The following analysis was performed on PRCS Test #7. This data is shown in the accompanying plot in Figure 6-B. Analysis indicated that maximum motion of the Spektr array occurred just after the thruster firings and was on the order of 3 inches. Note that the motion appears to be in the form of a damped sinusoid. The data also implies the existence of a dominant frequency peak, which can be clearly seen in Figure 6-C.

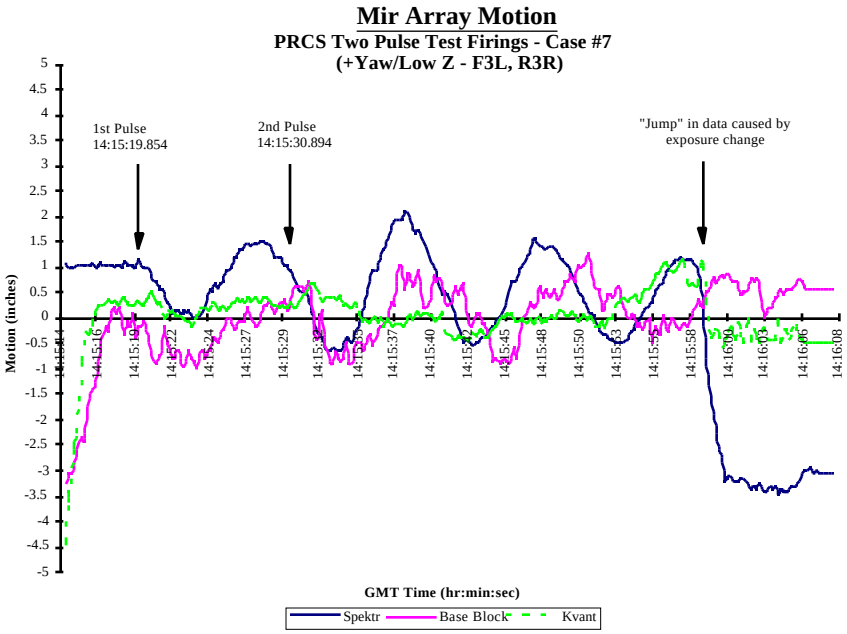

Figure 6-B Array Motion from PRCS Test #7

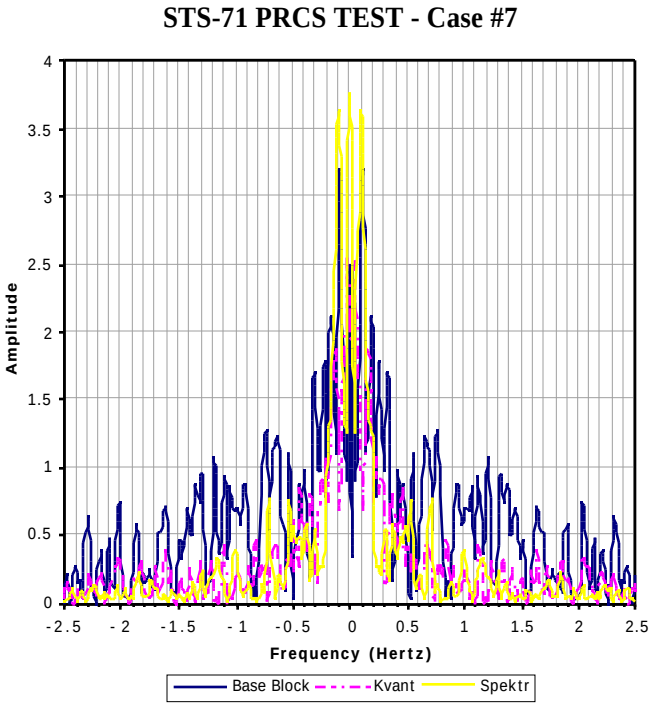

Figure 6-C Frequency Analysis from PRCS Test #7

Test	*# Pulses Motion*	*Shuttle RCS Jets*	*GMT Time*	*Max. Amplitude (inches)*			*Peak frequencies (Hertz)*		
				Sp	**BB**	**Kv**	**Sp**	**BB**	**Kv**
1	**Single Pulse -Pitch**	L3D, R3D	182:12:35:32.094	0.5	2.0	0.5	none	0.100	0.150
2	**Single Pulse +Pitch**	F3D, F4D	182:12:38:02.494	1.0	0.5	0.5	0.050	0.100	0.075
3	**Single Pulse -Yaw**	F4R, L1L	182:12:40:02.494	2.0	2.0	2.0	0.150	0.150	0.050 0.150
4	**Single Pulse -Roll**	F3L, F3D	182:12:43:32.814	n/a	2.0	0.5	n/a	0.200	0.050
5	**Two Pulse +Pitch**	F3D, F4D	182:14:11:19.694 182:14:11:30.734	0.5	3.5	2.0	0.100	0.100	0.025 0.150
6	**Two Pulse +Pitch**	L3D, R3D	182:14:13:20.334 182:14:13:31.374	0.0	0.5	0.0	0.025	0.025 0.100	0.050
7	**Two Pulse +Pitch**	F3L, R3R	182:14:15:19.854 182:14:15:30.894	3.0	2.0	0.5	0.100	0.025 0.100	0.050
8	**Two Pulse +Pitch**	F4R, F4D	182:14:16:31.374 182:14:16:42.414	n/a	2.0	0.5	n/a	0.100	0.025 0.100 0.175 0.275

Table 6-A Analysis of PRCS Test Video Data

The maximum amplitude designation in Table 6-A was determined from the first major peak-to-peak motion after the specified thruster firing(s). Sub-pixel accuracies in the edge tracking algorithm imply that scaling factors are the primary source of error in the data. This error is on the order of +/- 0.5 inches for the motion results.

Dominant frequencies were derived in the interpretation of frequency-domain plots generated from each test. Some subjective judgment was made in the selection of peaks, since higher frequencies are often associated with noise in the data. Primary sources of error in the interpretation of this frequency data are the resolution of the output plot (+/- 0.025 Hertz) and the resulting peak selection procedure.

All of the PRCS data plots are included in Appendix C. A summary of results obtained from analysis of the video test data is shown in Table 6-A. The 'Sp', 'BB' and 'Kv' in the table refer to the Spektr, Base Block and Kvant arrays respectively.

Examination of the results presented in Table 6-A leads to the following statements:

- Test #3 (1-pulse, -yaw) and #5 (2-pulse, +pitch) caused the most Kvant array motion.
- Test #5 (2-pulse, +pitch) caused the most Base Block array motion.
- Test #7 (2-pulse, +pitch) caused the most Spektr array motion.
- Test #6 (2-pulse, +pitch) caused the least array motion.
- Test #3 (1-pulse, -yaw) was the only test where a common frequency was found for all arrays (0.150 Hertz).

7. MOTION ANALYSIS FROM VIDEO

A test to evaluate the accuracy of photographic and video data in calculating distance from the Shuttle to the Mir was performed. Trajectory Control System (TCS) data available during the rendezvous served as ground truth for the analysis. TCS accuracy decreases as a function of separation distance.

Video and still photography coverage of the Mir from the Shuttle during approach, fly-around and backaway was reviewed. Measurements were made from both video and still footage to determine the relative motion between the Shuttle and Mir during approach, fly-around, and backaway. Still photography data was collected from both 35 mm and 70 mm film. However, uncertainties about the lenses used during the approach and backaway procedures precluded the use of still photography in this comparison. However, the video measurements were compared with the TCS data.

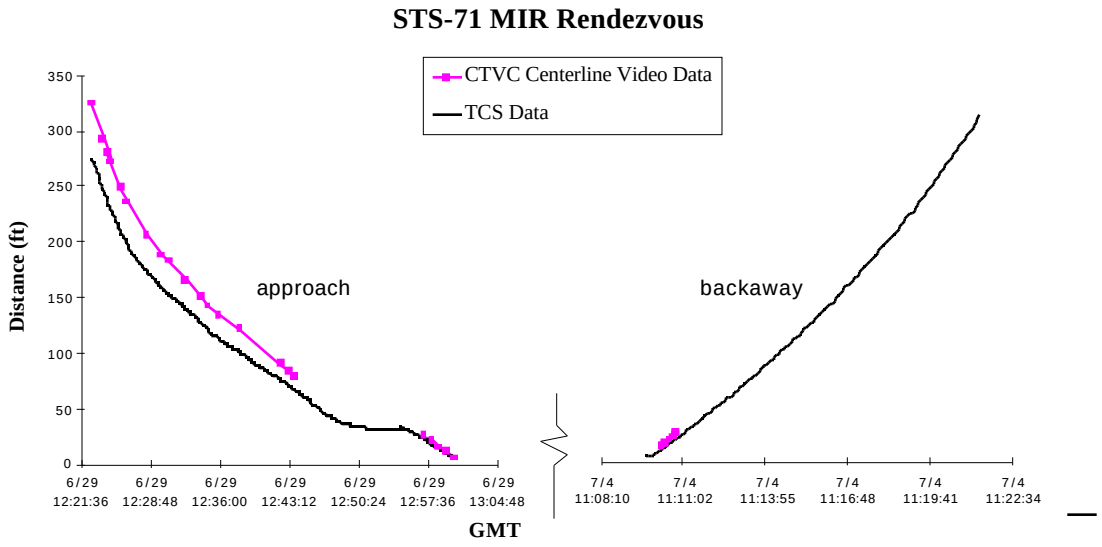

Figure 7-A Orbiter to Mir Distance using TCS and Centerline Video Data

Figure 7-A compares actual TCS data with that from the ODS centerline video camera. Camera distance calculations utilized horizontal-field-of-view (HFOV) information embedded in the vertical interval. The HFOV numbers have +/- 1° errors, and when propagated through photogrammetric equations, result in maximum errors of +/- 20%. As seen in Figure 7-A, video data was not acquired through portions of the approach and backaway sequences.

8. IMAGERY EVALUATION

This section discusses overall quality of the film and video data. A scenelist documenting Mir survey subject matter by specific rolls is included in Appendix E. Information on how to obtain a detailed video scenelist of STS-71 is in Appendix F.

Imagery acquired of Mir surfaces during STS-71 consisted of the following:

- 15 hours of downlink video
- 9 hours of onboard video
- 215 frames of 35 mm film
- 435 frames of 70 mm film
- 50 Electronic Still Camera (ESC) images

8.1 Video Review

The CTVC camera in the centerline position provided good views from far approach through thirty minutes prior to docking. Recorder problems prevented acquisition of the last thirty minutes of approach from the centerline camera. However, a multiplexed image showing split views from PLB camera A and the centerline camera was downlinked the last few minutes of approach. Excellent coverage of the far approach was obtained from PLB camera B. This zoomed-in view allowed assessment of the Base Block solar array impingement while the Shuttle was at a range between 500 and 1000 feet. Short clips of the approach procedure were obtained from the aft PLB camera C.

Much of the downlinked survey video was obtained via INCO ground control during the initial two crew sleep periods of the docked phase. This footage provided excellent coverage of the Orbiter-facing sides of the Spektr and Kvant-2 modules, as well as most of the Kristall docking module. Solar array coverage was spotty at best, since imagery was generally limited to viewing array undersides (due to the position of the sun). The CTVC cameras at positions B and D were used to acquire imagery of Spektr, Base Block, and Kvant solar array motion during the Primary Reaction Control System (PRCS) test. The fields-of-view for both cameras were sufficient to perform motion and frequency analysis. However, video acquired of the lower Spektr array displayed blooming characteristics during several of these tests and settings were not optimized. Camcorder video was primarily limited to flight deck views of crew rendezvous activities.

The centerline camera provided good views of the Mir's docking interface area during the first minute of backaway. After that time, the sun was pointing directly at the camera for much of the backaway and hampered analysis. Camera A provided coverage of the initial backaway sequence and showed the orientation of the Spektr arrays at the time of undocking.

Fly-around data included imagery where the Mir Station filled the field-of-view. Centerline CTVC camera footage included scenes where the Base Block and Kvant modules were visible. Part of the fly-around was not captured on video due to darkness.

In general, payload bay camera views provided good overview imagery of the station configuration. Notable exceptions to this were detailed imagery of the docking mechanism during the final approach and the initial backaway. The CTVC cameras and their

corresponding settings also provided excellent imagery during the docked phase survey of the Mir Station.

TYPE	*Approach*	*Docked (survey)*	*Docked (PRCS test)*	*Backaway*	*Fly-around*
Downlink (tape ID #)	8,9	10,11,12,13, 14,15,16	19, 20	32	33
Onboard (tape ID #)	1,5,7	27	16,18	28	31, 32, 33

Table 8-A Onboard Video Coverage of Mir Rendezvous Events

Table 8-A summarizes the event coverage recorded onto different downlink and onboard tapes. Note that some downlink scenes may be overlapped by those on the onboard video.

8.2 Still Photography Review

Views of the Mir docking mechanism were acquired using the Hasselblad (70 mm) camera during approach. Lighting conditions and overhead window access hampered data acquisition during this time period.

Systematic coverage of the Orbiter-facing sides of the Spektr, Kvant-2 and Kristall modules were obtained using the Hasselblad during the docked phase. Several views of the partially unfurled Spektr array were acquired. Imagery acquired using the Hasselblad with a 250 mm lens revealed discoloration and small anomalies on the surface of the Kvant-2 and Kristall modules. Due to available view angles and sun position, detailed photographic coverage of the solar panels was limited to the Kvant arrays. Some close-up views of the folded Kvant-2 array, along with an adjacent bowed array, were acquired. The color and black and white Electronic Still Cameras (ESC) were used to obtain images of the partially unfurled Spektr solar array .

A few images of the docking mechanism area were obtained during backaway. Much of this phase was spent with the Mir directly between the Orbiter and the Sun and the resultant glare severely hampered data acquisition.

Fly-around imagery showed the side of the Mir Base Block opposite that seen during STS-63. A panel, similar to those identified as micrometeoroid sensors on STS-63, was visible on the Base Block. Discoloration was seen on the exterior surfaces of both the Base Block and the Kvant modules.

Whereas more still photography was acquired on STS-63, the detail achieved on STS-71 was excellent. This was partially due to having more time available to set up cameras and perform systematic coverage of the Orbiter-facing sides of the Kvant-2, Kristall and Spektr modules. The orientation of the Mir during the docked sequence minimized the amount of imagery obtained on the Base Block and Kvant modules. Also, poor lighting conditions at the time of backaway severely limited acquisition of usable data during that phase. The availability of color and black and white ESC cameras afforded crew members the opportunity to acquire and downlink views prior to target acquisition with film cameras.

TYPE	*Approach*	*Docked (survey)*	*Soyuz undock*	*Backaway*	*Fly-around*
Hasselblad (Roll #)	701, 702, 723	702, 704, 723, 741, 742	704, 741	704	741, 744
Nikon (Roll #)		101, 103, 104, 107, 117, 321, 329, 330, 389	126		
ESC		all			

Table 8-B Still Photography Coverage of Mir Rendezvous Events

Table 8-B summarizes the event coverage recorded by the different still photography sources. Note that the specified rolls contain coverage of Mir external surfaces that may be in addition to other footage.

8.3 ESC / Nikon Image Comparison

A scheduled test to perform a quantitative comparison between the ESC and Nikon film cameras was scrubbed due to crew time constraints. An assumption was made that such a test would be a "real-world" application to compare and contrast the differences between the two media. Although some common targets were obtained on both the digital and film imagery, sun angles and camera configurations were not fixed. A representative image pair is shown below in Figures 8-A and 8-B.

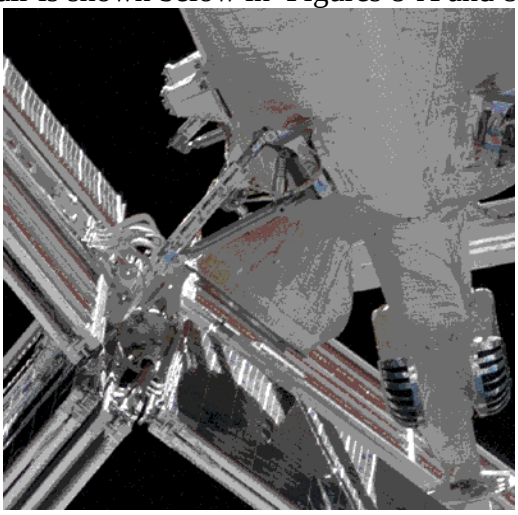

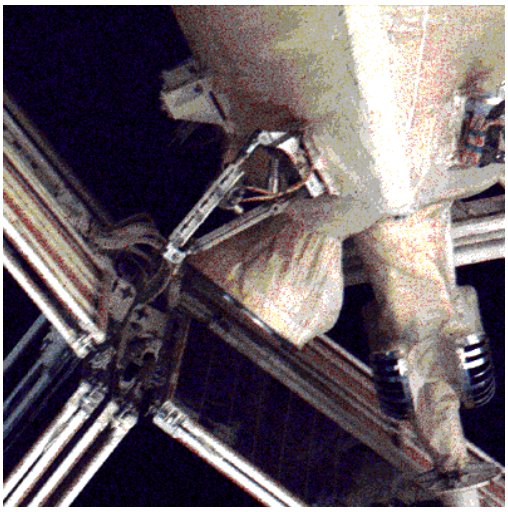

Figure 8-A Nikon view of Spektr Array **Figure 8-B ESC view of Spektr Array**

A subjective comparison of the images in Figures 8-A and 8-B indicate that the ESC, while suitable for quick look analysis, does not approach the resolution of the film camera. A more rigorous test may be conducted on a future mission as crew time and training procedures allow.

9. CONCLUSIONS AND RECOMMENDATIONS

9.1 Conclusions

Data gathered from the STS-71 rendezvous provides baseline coverage of both the Kvant-2 and Spektr modules. Imagery collected from the STS-63 and STS-71 missions provide significant data points from which an assessment can be made of the effect of the space environment on an orbiting platform.

9.1.1 Discussion of Results

The information gathered during the STS-71 Mir survey complemented that from STS-63. The level of detail acquired on the Orbiter-facing sides of the Kvant-2 and Spektr modules matched expectations that were based on STS-63 imagery detail. Imagery of one of the Kvant arrays revealed several instances where cells appeared to be peeling off. Since this type of damage was not visible during the limited coverage gathered during STS-63, the anomalies may have occurred when the array was relocated to Kvant from the Kristall module. It is also interesting to note that anomalies seen on other arrays appear to be caused by impact damage, whereas these do not. Another item of interest from the analysis of film data is that the photography tended to wash out what may have been anomalies on pure white surfaces unless the exposures have been set to view those specific areas. Future detailed photography will need to emphasize that exposures be set for the specific region of interest, even if the field-of-view encompasses a larger area.

Survey video data was mainly used for the study of motion. Unlike STS-63, when crew time constraints precluded acquisition of plume impingement data, there were no braking pulses applied during the final approach sequence on STS-71 that might have resulted in array motion. However, views of the station during far approach did reveal Base Block array motion while the station was rotating into its docking configuration. Since this motion was unexpected, further study during future missions is warranted and will be emphasized. Finally, the PRCS video analysis was performed so that plume impingement specialists could correlate visual data with accelerometer data. Information from these tests can be used to verify structural dynamics models of the Shuttle/Mir docked configuration.

9.1.2 Assessment of DTO-1118 Procedures

Based on lessons learned from the STS-63 data, several procedures had been modified for the collection of data on STS-71. The most significant of these changes was using the Hasselblad camera as the primary means of acquiring still photography. This was necessary to obtain the larger fields-of-view, and thus, more reference information when performing detailed surveys. Also, a systematic technique to acquire imagery of the different modules was implemented during STS-71. The following conclusions can be drawn from analyzing procedures and equipment used to acquire the film and video data:

- Quality of both the 70mm and 35mm still photography was excellent.
- Crew time limitations limited the quantity of still photography acquired.
- Imagery acquired of the docking mechanism area during approach and backaway were only adequate due to sun glare problems.

- Blemishes on pure white surface features such as radiators and tanks were difficult to acquire with photography.
- Sun glare during backaway precluded acquisition of plume impingement data.
- Payload bay video camera settings were not optimized during the PRCS tests.
- Zoomed-in payload bay camera 'B' view during the far approach allowed detection of unexpected Mir Base Block solar panel motion.
- The limited amount of camcorder footage of Mir exterior surfaces was not useful for analysis.
- Use of INCO controlled payload bay cameras to perform surveys during sleep periods minimized crew impact.
- ESC imagery was adequate for quick-look analysis, but did not appear to provide detail for in-depth analysis.

9.2 Recommendations

STS-74 is the next Mir rendezvous mission. Current plans call for a station-keep at 170 feet. This should allow acquisition of image data while the Mir orients the docking module toward the Orbiter. Based on investigator inputs during the STS-71 imagery review and crew comments during STS-74 training, the following recommendations have been made:

- Include more camera field-of-view diagrams in the Flight Data File.
- Highest priority remains obtaining still imagery of the docking mechanism both prior to docking and after undocking.
- Continue to utilize ground control of payload bay video cameras to perform Mir surveys during crew sleep periods.
- Request five daylight passes (assuming 1 crew member) to collect desired information for the survey.
- Understand lighting condition as a function of the rendezvous timeline and its corresponding effect on image acquisition.
- Emphasize using exposure settings for the bright areas (such as radiators and tanks) within a region of interest rather than the entire field-of-view.
- Determine the usefulness of the Mir attitude orientation maneuver as compared to the fly-around for survey imagery.

10. REFERENCES

- Bluth Ph.D., B. J., D. Fielder, Soviet Space Stations as Analogs, Vol. II, 3rd Edition, September 1993.
- Gaskill, J. D., *Linear Systems, Fourier Transforms, and Optics*, John Wiley & Sons, New York, New York, 1978.
- Lillesand, T. M., R. W. Kiefer, *Remote Sensing and Image Interpretation*, John Wiley & Sons, New York, New York, 1979.
- NASA/RSC-E Joint Report, Mir Photo/TV Survey (DTO-1118): STS-63, JSC-27246, August 28, 1995.
- Mission Operations Directorate, Space Flight Training Division, Systems Training Branch, A Russian Space Station: The Mir Complex, National Aeronautics and Space Administration, Lyndon B. Johnson Space Center, Houston, Texas, February 1994.
- NASA Drawing Package, STS-71 Shuttle Mir Docking Mission, WG-3/NPO-E/NASA/003/3402-1, March, 24 1995.
- Portree, David S. F., Information Services Division, Mir Hardware Heritage, JSC 26770, Lyndon B. Johnson Space Center, Houston, Texas, October 1994.

APPENDICES

Appendix A: STS-71 Mir Surface Damage / Discoloration

The following table summarizes the damage and discoloration observed on the Mir station as seen during STS-71. All visible module, capsule, and array surfaces were examined for anomalies, and where possible, measurements were obtained. In addition to identifying locations of damage, the table also lists the specific frames from which measurements were obtained. Damage features previously seen on STS-63 are also documented.

Appendix B: DTO-1118 Mir Surface Coverage Status

The accompanying images document surface coverage resulting from the photographic and video surveys performed on STS-63 and STS-71. Cumulative coverage seen from these two missions provides a baseline from which future surveys will document new anomalies.

STS-63 provided good coverage of the orbiter-facing sides of the Base Block and Kvant modules. STS-71 provided detailed coverage of the orbiter-facing sides of the Kvant-2 and Spektr modules, along with some of the Kristall module. Detailed coverage of the docking mechanism was obtained on both missions.

Upcoming rendezvous missions (STS-74 and STS-76) will provide an opportunity to view the Kvant-2, Spektr, and Kristall modules in detail to further evaluate the effect of the space environment on specific material surfaces.

Two pairs of surface coverage imagery are included. The first pair documents coverage resulting from the STS-63 mission. The second pair shows the cumulative surface coverage resulting from both the STS-63 and STS-71 missions.

Appendix C: STS-71 PRCS Video Analysis Plots

Onboard (ID 609764, #16) and downlink (ID 609677, orbits 58, 59, 60) video were used in the PRCS analysis. Four single pulse and four double pulse tests were performed to determine the effect of Shuttle thruster firings on the docked configuration. Results of each data set (summarized in Table 6-A) is presented in the following motion and frequency plots.

Appendix D: Retrieved Centerline Target Photo Survey

The docking target installed on the Kristall module prior to STS-63 was replaced on STS-71. The new docking target is supposed to allow easier reading of angular alignment offsets during approach procedures.

A detailed photographic survey was performed on the retrieved target after it was returned to JSC. The following images are meant to show the type of damage and discoloration observed on the target surface.

- The photograph at the top left corner is a general view with arrows that point to anomalies on the surface that might be attributed to possible impacts.
- The adjacent image is one where color balance levels have been enhanced to identify areas of discoloration on the target. This image should only be used for relative comparisons within the target since it has been enhanced for viewability purposes.
- The bottom image zooms in on an area within the target to show the type of impact damage visible on the surface.

Appendix E: STS-71 Film Scenelist

The following subset of the STS-71 film scenelist was compiled by the Imagery Services Branch/PS4 and breaks down coverage of Mir items on each roll of 35mm and 70mm films.

Correlation of specific rendezvous events to rolls of film are documented in Table 9-B.

Appendix F: STS-71 Video Scenelist Information

The following information on acquiring video scenelist information was compiled by the Imagery Services Branch/PS4.

Correlation of specific rendezvous events to tape identification numbers are documented in Table 9-A.

Appendix G: STS-71 Camera Layout

The following image describes the layout of film and photographic equipment specific to Mir survey events during the STS-71 rendezvous.

Appendix H: Acronym List

APDU	Androgynous Peripheral Docking Unit
CAD	Computer Aided Design
CTVC	Color Television Camera
DTO	Detailed Test Objective
ESC	Electronic Still Camera
EVA	Extra Vehicular Activity
FFT	Fast Fourier Transform
GMT	Greenwich Mean Time
HEI	Hernandez Engineering Inc.
HFOV	Horizontal-Field-Of-View
INCO	Instrumentation and Communication Office
IS&AG	Image Science & Analysis Group
ISS	International Space Station
JSC	Johnson Space Center
LMES	Lockheed Martin Engineering and Sciences
NASA	National Aeronautics & Space Administration
ODS	Orbiter Docking System
PLB	Payload Bay
PRCS	Primary Reaction Control System
RCS	Reaction Control System
RSC-E	Russian Space Center-Energia
RSO	Rockwell Space Operations
STS	Space Transportation System
TCS	Trajectory Control System